

1 Title: History of previous midlife estradiol treatment permanently alters interactions of brain
2 insulin-like growth factor-1 signaling and hippocampal estrogen synthesis to enhance cognitive
3 aging in a rat model of menopause

4 Abbreviated title: Prev E alters brain ER signaling to enhance cog aging

5 Authors: Nina E. Baumgartner^{1,2}, Shannon M. McQuillen^{1,2}, Samantha F. Perry^{1,2}, Sangtawan
6 Miller^{1,2}, Robert Gibbs⁴, Jill M Daniel^{1,2,3}

7 ¹Brain Institute ²Neuroscience Program ³Department of Psychology, Tulane University, New
8 Orleans, LA 70118; ⁴Department of Pharmaceutical Sciences, University of Pittsburgh School of
9 Pharmacy, Pittsburgh, PA 15261.

10 Corresponding author: Nina E. Baumgartner, nbaumgar@tulane.edu

11 Number of pages: 54

12 Number of figures: 10

13 Abstract word count: 250

14 Introduction word count: 650

15 Discussion word count: 1400

16 Conflicts of interests: The authors report no conflicts of interest.

17 Acknowledgements: This work was supported by the National Institute on Aging Grant

18 RF1AG041374 to JMD. In addition, this project used the services of the University of Pittsburgh

19 Small Molecule Biomarker Core, which was partially funded by NIH through S10RR023461 and

20 S10OD028540.

21 Dedication: We dedicate this manuscript to Jefferson J. Huggins (1988-2020), who assisted with
22 behavioral tests for this manuscript. More importantly, his intellectual curiosity and sense of
23 wonder made a lasting impact on the authors.

24 **Abstract**

25 Across species, including humans, elevated levels of brain estrogen receptor (ER) α are
26 associated with enhanced cognitive aging even in the absence of circulating estrogens. In
27 rodents, short-term estrogen treatment—such as that commonly used in the menopausal
28 transition—results in long-term increases in levels of ER α in the hippocampus, leading to
29 enhanced memory long after termination of estrogen treatment. However, mechanisms by
30 which increased levels of brain ER α enhances cognitive aging remain unclear. Here we show
31 that in the hippocampus, insulin-like growth factor-1 (IGF-1)—which can activate ER via ligand-
32 independent mechanisms—requires concomitant synthesis of brain-derived neuroestrogens to
33 phosphorylate ER α via MAPK signaling, ultimately resulting in enhanced memory. In a rat model
34 of menopause involving long-term ovarian hormone deprivation, hippocampal neuroestrogen
35 activity decreases, altering IGF-1 activity and resulting in impaired memory. However, this
36 process is reversed by short-term estradiol treatment. Forty-days of estradiol exposure following
37 ovariectomy results in maintenance of neuroestrogen levels that persist beyond the period of
38 hormone treatment, allowing for continued interactions between IGF-1 and neuroestrogen
39 signaling, elevated levels of hippocampal ER α , and ultimately enhanced memory. Collectively,
40 results demonstrate that short-term estradiol use following loss of ovarian function has long-
41 lasting effects on hippocampal function and memory by dynamically regulating cellular
42 mechanisms that promote activity of ER α in the absence of circulating estrogens. Translational
43 impacts of these findings suggest lasting cognitive benefits of short-term estrogen use near
44 menopause and highlight the importance of hippocampal ER α —independent from the role of
45 circulating estrogens—in regulating memory in aging females.

46

47

48

49 **Significance statement**

50 Declines in ovarian hormones following menopause coincide with increased risk of
51 cognitive decline. Due to potential health risks, current recommendations are that menopausal
52 estrogen therapy be limited to a few years. Long-term consequences for the brain and memory
53 of this short-term midlife estrogen therapy are unclear. Here, in a rodent model of menopause,
54 we determined mechanisms by which short-term midlife estrogen exposure can enhance
55 hippocampal function and memory with cognitive benefits and molecular changes enduring long
56 after termination of estrogen exposure. Our model indicates long-lasting benefits of maintaining
57 hippocampal estrogen receptor function in the absence of ongoing estrogen exposure and
58 suggests potential strategies for combating age-related cognitive decline.

59

60

61 **Introduction**

62 Loss of ovarian hormones during menopause coincides with cognitive decline and
63 increased risk of age-related dementias (Henderson et al. 1996; Sherwin 1994). Due to putative
64 health risks associated with prolonged estrogen exposure, current health guidelines recommend
65 using menopausal estrogen treatment for as short a time as possible. Work from our lab in a
66 rodent model of menopause has demonstrated long-lasting benefits of short-term midlife
67 estradiol treatment on hippocampal function and memory through sustained activation of
68 estrogen receptor (ER) α that are likely permanent, persisting long after estradiol treatment is
69 terminated (Rodgers et al 2010; Witty et al 2013; Black et al. 2016; Baumgartner et al. 2021).
70 These findings correspond with evidence across multiple species, including humans, that
71 elevated levels of brain estrogen receptor ER α are associated with enhanced cognitive aging
72 even in the absence of circulating estrogens (For review, see Baumgartner and Daniel, 2020).
73 The mechanisms by which increased levels of brain ER α enhance cognitive aging following
74 previous midlife exposure to estradiol are unclear.

75 Short-term exposure to estradiol in midlife enhances memory and increases levels of
76 hippocampal ER α long-term in ovariectomized rodents (Rodgers et al. 2010), effects dependent
77 on insulin-like growth factor-1 (IGF-1) signaling (Witty et al. 2013) and resulting in sustained ER-
78 dependent transcriptional activity (Pollard et al. 2018). IGF-1 is a peptide hormone that acts
79 through IGF-1R, a tyrosine kinase receptor with much functional overlap with ER α , including
80 activation of MAPK and PI3K-AKT signaling pathways by both receptors (Russo et al. 2005;
81 Sohrabji 2015). ER α and IGF-1R co-localize and form estradiol-dependent protein complexes in
82 the hippocampus (Cardona-Gomez et al. 2000; Mendez et al. 2003). Implications for these
83 subcellular interactions for cognition remain to be determined. IGF-1 administration activates
84 ER α via ligand-independent mechanisms *in vitro* (Kato et al. 1995) and in recently
85 ovariectomized rats via phosphorylation at serine-118 (Grissom and Daniel 2016), a phospho-

86 site crucial for protecting ER α from degradation (Valley et al. 2005). An *in vitro* study revealed
87 that neuroestrogen synthesis is required for IGF-1-mediated activation of ER α , potentially
88 through synergistic activation of the MAPK pathway (Pollard and Daniel 2019).

89 Contradicting a potential role for neuroestrogens in activation of ER α following loss of
90 ovarian function are data indicating that hippocampal neuroestrogens are regulated by
91 circulating estrogens (Nelson et al. 2016) and demonstrations of decreases in hippocampal
92 aromatase expression and neuroestrogen levels following long-term ovariectomy (Chen et al.
93 2021; Ma et al 2020). Additionally, we showed that blocking neuroestrogen synthesis via
94 aromatase inhibition had no impact on hippocampal ER-dependent transcription in long-term
95 ovariectomized mice (Baumgartner et al 2019). Collectively, these data point to a diminished
96 role for neuroestrogen synthesis in hippocampal function following long-term ovarian hormone
97 deprivation.

98 In summary, data indicate that a history of midlife estradiol treatment impacts memory
99 long after termination of estradiol treatment through lasting activation of hippocampal ER α by
100 ligand-independent mechanisms via IGF1-signaling. *In vitro* evidence indicates that ligand-
101 independent activation of ER by IGF-1 requires concomitant neuroestrogen synthesis. However,
102 neuroestrogen levels in the hippocampus are diminished following long-term loss of ovarian
103 hormones. The goal of the current work was to reconcile these contradictory findings and
104 determine implications for female cognitive aging following loss of ovarian function of the
105 interactive actions of IGF-1 and neuroestrogens and determine if history of estradiol use
106 impacts that interaction. First, we determined the necessity of neuroestrogen synthesis in the
107 ability of IGF-1 to activate ER α *in vivo* via its downstream signaling pathways and subsequent
108 impact on memory. Next, we determined if interactions of neuroestrogens and IGF-1 in the
109 hippocampus and subsequent impact on memory were altered in two models of menopause—
110 one with and one without a history of past midlife estradiol use. Our findings provide a potential
111 model for combatting postmenopausal cognitive decline in which short-term estradiol treatment

112 following the loss of ovarian hormones sustains hippocampal function and memory well beyond
113 the period of estradiol exposure by permanently altering the dynamic relationship between IGF-
114 1R signaling and neuroestrogen synthesis.

115

116 **Materials and Methods**

117 *Subjects*

118 Middle-aged female Long-Evans hooded rats (Envigo), retired breeders (~11 months of
119 age), were used for all experiments. Animal care was in accordance with guidelines set by the
120 National Institute of Health Guide for the Care and Use of Laboratory Animals and all
121 procedures were approved by the Institutional Animal Care and Use Committee of Tulane
122 University. Rats were housed individually in a temperature-controlled vivarium under a 12-h
123 light, 12-h dark cycle and had unrestricted access to food and water unless otherwise noted.

124

125 *Ovariectomies and hormone treatments*

126 All rats in experiments were anesthetized by intraperitoneal injections of ketamine (100
127 mg/kg ip; Bristol Laboratories, Syracuse, NY) and xylazine (7 mg/kg ip; Miles Laboratories,
128 Shawnee, KS) and ovariectomized. Buprenorphine (0.375 mg/kg; Reckitt Benckiser Health
129 Care) was administered by subcutaneous injection before the start of each surgery.

130 Ovariectomy surgery involved bilateral flank incisions through the skin and muscle wall and the
131 removal of ovaries.

132 For Experiments 3 and 4, rats were implanted with a subcutaneous 5-mm SILASTIC
133 brand capsule (0.058 in. inner diameter and 0.077 in. outer diameter; Dow Corning, Midland,
134 MI) on the dorsal aspect of the neck immediately following ovariectomy. Capsules contained
135 either cholesterol vehicle (Experiment 3; Sigma-Aldrich, St. Louis, MO) or 25% 17 β -estradiol
136 (Experiment 4; Sigma-Aldrich) diluted in vehicle. We have previously shown that implants of
137 these dimensions and estradiol concentrations maintain blood serum estradiol levels in middle-

138 age retired breeders at approximately 37 pg/mL (Bohacek & Daniel 2007), which falls within
139 physiological range. Forty days after ovariectomy and capsule implantation, capsules were
140 removed. Vaginal smears for each rat were collected for at least four consecutive days before
141 capsule replacement in order to confirm hormone treatment for the initial forty-day window.
142 Smears of ovariectomized, cholesterol-treated rats were characterized by a predominance of
143 leukocytes, while smears of ovariectomized, estradiol-treated rats were characterized by a
144 predominance of cornified and nucleated epithelial cells.

145

146 *Stereotaxic surgeries*

147 Rats were anesthetized with ketamine and xylazine as described above and
148 administered buprenorphine as an analgesic. Rats were then placed into a stereotaxic frame.
149 An incision was made in the scalp and fascia that overlie the skull and a hole was drilled in the
150 skull.

151 In Experiment 1, a cannula connected to a Hamilton syringe via silastic tubing was
152 lowered through the hole to the appropriate depth to reach the right lateral ventricle (relative to
153 bregma: anteroposterior, -0.5 mm; mediolateral, -1.1 mm; dorsoventral, -2.5 mm). Cannulas
154 delivered 5 μ L of either vehicle containing 8% DMSO (Sigma-Aldrich) in aCSF (Tocris), 2 μ g of
155 human IGF-1 (GroPep) diluted in vehicle, or 2 μ g of IGF-1 combined with 0.4 μ g of aromatase
156 inhibitor Letrozole (Sigma-Aldrich) diluted in vehicle over the course of 10 minutes.

157 In Experiments 2-4, a cannula (brain infusion kits, Alzet) was lowered through the hole to
158 the appropriate depth to reach the right lateral ventricle (relative to bregma: anteroposterior,
159 -0.3 mm; mediolateral, -1.2 mm; dorsoventral, -4.5 mm) and adhered to the skull with an
160 anchoring screw, Super Glue, and dental acrylic. The cannula was connected to an osmotic
161 mini-pump (flow rate, 0.15 μ L/h; Alzet) by vinyl tubing for drug delivery. Rats in Experiment 2
162 received mini-pumps that delivered either vehicle containing 6.7% DMSO in aCSF, human IGF-
163 1 (0.33 μ g/ μ L) diluted in vehicle, or human IGF-1 (0.33 μ g/ μ L) and letrozole (0.066 μ g/ μ L) diluted

164 in vehicle. Rats from Experiments 3 and 4 received mini-pumps that delivered either vehicle (8%
165 DMSO in aCSF), IGF-1 receptor antagonist JB1 in vehicle (300 µg/mL, Bachem), aromatase
166 inhibitor letrozole in vehicle (0.066 ug/ul), or both JB1 + letrozole in vehicle.

167

168 *Radial-arm maze training*

169 Approximately one week before the start of behavioral training, rats were food restricted
170 and weighed daily to maintain their body weights at 85-90% of their free-feeding weight. Rats
171 then began training on the 8-arm radial-maze task (Coulbourn Instruments, Whitehall, PA), as
172 previously described (Daniel 2015). The maze consists of eight arms (66 cm long × 9.5 cm wide
173 × 11.5 cm high) with a metal grated floor and clear acrylic walls. Arms extend out radially from a
174 central hub that is 28 cm in diameter and the maze was placed on a table that is approximately
175 1 m above the ground. The maze was centered in a 3 × 5 m room with many visible extra maze
176 cues. During training, a single food reward (Froot Loops; Kellogg Co., Battle Creek, MI) was
177 placed in an opaque dish, 5.5 cm in diameter and 1.25 cm tall, at the end of each arm so it was
178 not visible from the center of the maze. For each trial, the rat was placed in the center of the
179 maze facing one of the eight arms. The starting orientation varied pseudo-randomly across
180 trials. The rat was then allowed to enter arms and obtain food rewards until all eight arms had
181 been visited or five minutes had elapsed. An arm entry was scored when all four paws crossed
182 the midline of the arm. The arm entry sequence was scored in real time by an observer located
183 in a fixed location in the room. Errors were scored if the rat re-entered an arm that had already
184 been visited previously in the trial. Rats were trained with one trial per day, five days per week,
185 for up to twenty-five days until they reached criterion by scoring fewer than 2 errors for three
186 consecutive days. Once criterion was reached, rats underwent stereotaxic surgery and drug
187 delivery as described above.

188

189 *Delay testing on radial-arm maze*

190 One week after stereotaxic surgeries, rats were tested on delay trials. During testing,
191 delays of various lengths were imposed which required the rats to remember over an extended
192 period of time which arms had previously been visited. Rats were placed in the center of the
193 maze facing one of the eight arms and allowed to enter four unique arms during the pre-delay
194 trial. After four correct arm choices, rats were removed from the maze and placed in a holding
195 cage for the duration of the delay. Following the delay, rats were returned to the center of the
196 maze in the same orientation from the pre-delay trial. During this post-delay trial, rats were
197 allowed to explore the maze until the four remaining, still baited arms were visited or until 5
198 minutes had elapsed. Re-entries into previously visited arms were recorded as errors. Arm-
199 choice accuracy was measured by errors of eight, which represented the number of errors
200 included in the first eight arm choices collectively across the pre-delay and post-delay trials.
201 Rats received 2 days of habituation to a 1-min delay trial. Each subsequent delay was tested
202 across two consecutive days. Delays for each experiment were chosen based on the
203 performance of the rats during the training period and were increased in difficulty until at least
204 two experimental groups performed within one standard deviation from chance (2.7 errors of
205 eight). Means of errors of eight across both days of testing for each delay were analyzed.

206

207 *Euthanasia and tissue collection*

208 Rats were killed under anesthesia induced by ketamine and xylazine. The hippocampus
209 was dissected out and quick frozen on dry ice and stored at -80°C until further processing. A 1-
210 cm sample of the right uterine horn was collected from each rat and weighed to verify
211 ovariectomy status or hormone treatment at the time of euthanasia.

212

213 *Tissue processing and western blotting*

214 In Experiment 1, right hippocampi were processed for subcellular protein fractionation
215 and compartment-specific western blotting as previously described (Baumgartner et al. 2021).

216 Briefly, hippocampal tissue was homogenized using the PowerGen-125 handheld homogenizer
217 (Fisher), strained through Pierce Tissue Strainers, and separated into cytosolic, membrane, and
218 nuclear compartments using consecutive centrifugation steps of varying speeds and specialized
219 buffers obtained from a commercially available kit (Sub-Cellular Protein Fractionation Kit for
220 Tissues, ThermoFisher). Bradford protein assays were performed for each compartment
221 individually. Each sample diluted 1:1 with Laemmli Sample Buffer (BioRad) mixed with 350 mM
222 DTT, boiled for 5 min, and stored at -80°C until western blotting.

223 The left hippocampi in Experiment 1 and the right hippocampi in Experiments 2-4 were
224 processed for whole-cell western blotting. Tissue was sonicated using the Fisherbrand Model 50
225 Sonic Dismembrator (Fisher) in 10 µl/mg lysis buffer containing 1 mM EGTA, 1 mM EDTA, 20
226 mM Tris, 1 mM sodium pyrophosphate tetrabasic decahydrate, 4 mM 4-nitrophenyl phosphate
227 disodium salt hexahydrate, 0.1 µM microcystin, and 1% protease inhibitor cocktail (Sigma-
228 Aldrich). Samples were then centrifuged for 15 min at 1000 x g at 4°C. Bradford protein assays
229 were performed to determine the protein concentration of each sample. Each sample diluted 1:1
230 with Laemmli Sample Buffer (BioRad) mixed with 350 mM DTT, boiled for 10 min, and stored at
231 -80°C until western blotting.

232 Fifteen micrograms of cytosolic, membrane, and nuclear protein from each sample, or
233 25 µg of whole-cell protein from each sample, was loaded onto and separated on a 7.5% TGX
234 SDS-PAGE gel at 250 V for 40 minutes. Molecular weight markers (Precision Plus Protein
235 Standards, BioRad) were included with each run. Proteins were transferred from gels to
236 nitrocellulose membranes at 100 V for 30 minutes. Membranes were blocked with 5% bovine
237 serum albumin (BSA) in 1% Tween 20/Tris-buffered saline (TTBS) with gentle mixing at room
238 temperature for 1 hour. After blocking, membranes were incubated with gentle mixing in primary
239 antibody overnight at 4°C in 1% BSA-TTBS. Samples from cytosolic, membrane, and nuclear
240 compartments were incubated with antibodies for phospho-S118 ERα (1:1000, Abcam) and
241 total ERα (1:1000, Santa Cruz). Samples from cytosolic fractions were incubated with antibodies

242 for cytosolic loading control Enolase (1:1000, Santa Cruz). Samples from membrane fractions
243 were incubated with antibodies for membrane loading control ATP1A1 (1:5000, ProteinTech).
244 Samples from nuclear fractions were incubated with antibodies for nuclear loading control
245 histone 3 (H3; 1:1000, Cell Signaling). Whole-cell tissue samples were incubated with
246 antibodies for phospho-MAPK (1:1000, Cell Signaling) and total p42-MAPK (1:1000, Cell
247 Signaling) which recognize both the p44- and p42-MAPK epitopes, phospho-Akt (1:1000, Cell
248 Signaling), total Akt (1:1000, Cell Signaling), total ER α (1:1000, Santa Cruz), aromatase
249 (1:1000, BioRad), or loading control GAPDH (1:1000, Santa Cruz). Following primary antibody
250 incubation, blots were washed three times for 15 minutes with TTBS. Blots were then incubated
251 with secondary antibodies conjugated to fluorophores in 5% BSA-TTBS for one hour at room
252 temperature with gentle mixing. Secondary antibodies used were StarBright B520 Rabbit
253 (BioRad; 1:5000 for p-S118 ER α , enolase, ATP1A1, H3, total MAPK, total Akt) and StarBright
254 B700 Mouse (BioRad; 1:5000 for total ER α , phosphor-MAPK, phospho-Akt, aromatase,
255 GAPDH). Blots were washed three times for 15 minutes with TTBS, and then imaged on the
256 ChemiDocMP set to channels for StarBright B520 and StarBright B700. MCID Core imaging
257 software was used to quantify optical density for bands of interest.

258

259 *Hippocampal estradiol detection*

260 Left hippocampi from Experiments 3-4 were processed for estradiol extraction and
261 measurement via UPLC-MS/MS as previously described and validated (Li et al 2016). This
262 method has recently been shown to sensitively detect estradiol levels in hippocampal tissue
263 from ovariectomized rats treated with estradiol in a dose-dependent manner (Li and Gibbs,
264 2019). Briefly, tissues were homogenized in a potassium phosphate buffer (0.12M, pH 7.4; 100
265 mg tissue/mL) containing 4.0 mM MgCl₂, 4.0 mM Tris and 50 mM sucrose. Samples were
266 spiked with deuterated 17 beta-estradiol and then extracted with n-butyl chloride (Sigma-Aldrich,
267 Inc). The organic layer was dried under nitrogen, then resuspended and derivatized with dansyl

268 chloride in a 1:1 mix of acetonitrile:water (pH 10.5, Sigma-Aldrich, Inc). Samples were then
269 centrifuged and the supernatant transferred to glass vials for UPLC-MS/MS analysis.
270 Calibration curves were prepared in a matrix of 0.2% 2-hydroxypropyl- β -cyclodextrin (HPCD)
271 and processed the same as the tissue extracts.

272 Estradiol was eluted using a Waters Acquity UPLC BEH C18, 1.7 μ m, 21 x 150 mm
273 reversed-phase column, with an acetonitrile:water (0.1% formic acid) gradient. Detection was in
274 the positive mode. Transitions used for analysis were 506->171 for estradiol, and 511->171 for
275 the internal standard. Note that this method is able to distinguish between 17-alpha and 17-
276 beta estradiol based on retention time. Limit of detectability is 0.009 pmol/mL (2.5 pg/mL) with
277 intra-day and inter-day relative standard deviations of less than 15% at all concentrations.

278

279 *Experimental Design and Statistical Analyses*

280 *Experiment 1.* Middle-aged rats were ovariectomized and 10 days later treated them with
281 an acute intracerebroventricular (icv) infusion of either vehicle, IGF-1, or IGF-1 plus letrozole, an
282 aromatase inhibitor that blocks estrogen synthesis. After one (Vehicle, n=9; IGF-1, n=9; IGF-1 +
283 Letrozole, n=10) or 24 (Vehicle, n=10; IGF-1, n=9; IGF-1 + Letrozole, n=9) hours, animals were
284 euthanized and hippocampi were dissected. Right hippocampal tissue was collected and
285 processed for subcellular fractionation and western blotting for phospho-S118 ER α and total
286 ER α . Left hippocampal tissue was collected and processed for whole-cell western blotting for
287 phospho-p42-MAPK/total p42-MAPK and phospho-Akt/total Akt to determine if blocking
288 neuroestrogen synthesis decreases MAPK and PI3K-Akt signaling in animals simultaneously
289 treated with IGF-1.

290 *Experiment 2.* Middle-aged rats were trained on the 8-arm radial maze for 21 days
291 before undergoing ovariectomy. Ten days after ovariectomy, rats were implanted with a cannula
292 and mini-pump which chronically delivered either vehicle (n=11), IGF-1 (n=9), or IGF-1 plus
293 letrozole (n=11) to the lateral ventricle for the duration of the experiment. Animals were then

294 tested on delay trials (1 min, 1hr, 3 hr, 4 hr, 5 hr) in the 8-arm radial maze to test hippocampal-
295 dependent spatial memory. Two days after the final day of delay testing, animals were
296 euthanized, and right hippocampal tissue was collected and processed for whole-cell western
297 blotting for phospho-p42-MAPK/total p42-MAPK and phospho-Akt/total to determine if chronic
298 letrozole treatment impacts hippocampal activation of the MAPK and PI3K-AkT pathways in
299 animals treated with IGF-1.

300 *Experiment 3.* Middle-aged rats were ovariectomized and immediately implanted with
301 subcutaneous vehicle capsules for forty days (to match subsequent estradiol treatments in
302 Experiment 4). Forty days later, capsules were removed. Animals were allowed to age for sixty
303 more days following capsule removal before behavioral training begin, resulting in a total of one-
304 hundred days between removal of estrogens (ovariectomy) and behavioral training. Following
305 that sixty-day waiting period, animals were trained on the radial-arm maze for 24 days. Animals
306 then underwent stereotaxic surgery and were implanted with a cannula and mini-pump that
307 chronically delivered either vehicle (n=10), IGF-1 receptor antagonist JB1 (n=10), aromatase
308 inhibitor letrozole (n=9), or JB1 and letrozole (n=9). Animals were tested on delay trials (No
309 delay, 1 min, 1 hr) in the radial-arm maze to test hippocampal-dependent spatial memory. Two
310 days after the final day of delay testing, animals were euthanized and right hippocampal tissue
311 was collected and processed for western blotting for ER α , aromatase, phospho-p42-MAPK, total
312 p42-MAPK, phospho-Akt, and total-Akt were performed. Left hippocampal tissues were
313 collected and processed for estradiol detection via UPLC-MS/MS.

314 *Experiment 4.* Middle-aged rats were ovariectomized and immediately implanted with
315 subcutaneous estradiol capsules. Forty days later, capsules were removed. Animals were
316 allowed to age for one-hundred more days following capsule removal before behavioral training
317 begin, resulting in a total of one-hundred days between removal of estrogens (capsule removal)
318 and behavioral training. Following the one-hundred day waiting period, animals were trained on
319 the radial arm maze for 24 days. Animals then underwent stereotaxic surgery and were

320 implanted with a cannula and mini-pump that chronically delivered either vehicle (n=9), IGF-1
321 receptor antagonist JB1 (n=8), aromatase inhibitor letrozole (n=9), or JB1 and letrozole (n=9).
322 Animals were tested on delay trials (No delay, 1 min, 1 hr, 2hr, 3hr) in the 8-arm radial maze to
323 test hippocampal-dependent spatial memory. Two days after the final day of delay testing,
324 animals were euthanized and right hippocampal tissue was collected and processed for western
325 blotting for ER α , aromatase, phospho-p42-MAPK, total p42-MAPK, phospho-Akt, and total-Akt
326 were performed. Left hippocampal tissue were collected and processed for estradiol detection
327 via UPLC-MS/MS.

328 *Statistical Analyses.* All data analyses were performed using SPSS software. Behavioral
329 data were analyzed by Mixed-Design ANOVA comparing Errors of 8 between treatment groups
330 and across delay trials. Subsequent post-hoc testing, as described below, was used as
331 appropriate for between-subject effects. Western blotting and mass spec data were analyzed by
332 One-Way ANOVA comparing optical density and estradiol levels in fmol/mL, respectively,
333 between experiment groups with subsequent post-hoc testing as appropriate.

334 For experiments with only three experimental groups (Experiment 1 and 2), LSD post-
335 hoc testing was used as appropriate for between-group effects. For experiments with more than
336 three experimental groups (Experiments 3 and 4), a significant main effect of treatment was
337 probed by the Dunnett's 2-sided post hoc test, which compares treatments with a single control
338 group (Vehicle group). Western data were analyzed by One-Way ANOVA comparing optical
339 density between treatment group and subsequent post-hoc testing as appropriate. For
340 quantification of estradiol levels, two samples from the Letrozole group in Experiment 3 were
341 used for spike and recovery tests to optimize procedures for these set of samples and were
342 therefore excluded from statistical analysis. Additionally, due to the high sensitivity of mass spec
343 detection, extreme statistical outliers as identified by SPSS software (defined as $\pm 3 \times$
344 interquartile range from the first or third quartiles for each group) were presumed to indicate
345 sample contamination and therefore were excluded from statistical analyses. Researchers were

346 blind to treatment group during behavioral testing, western blotting, mass spec, and data
347 analysis.

348

349 **Results**

350 Experiment 1: Neuroestrogen synthesis is necessary for IGF-1-mediated phosphorylation and
351 subsequent increase in protein levels of ER α in the hippocampus of recently ovariectomized
352 middle-aged rats.

353 In the absence of ovarian estrogens, IGF-1 activates ER α via ligand-independent
354 mechanisms (Kato et al. 1995; Grissom and Daniel 2016). IGF-1 activation of ER α *in vitro*
355 requires concomitant neuroestrogen synthesis (Pollard and Daniel 2019). The goal of this
356 experiment was to test the hypothesis that neuroestrogen synthesis is required for IGF-1
357 activation of ER α protein *in vivo*. Recently ovariectomized middle-aged received icv infusions of
358 either vehicle (Veh group), IGF-1 (IGF-1 group), or IGF-1 plus letrozole (IGF-1 + Let group).
359 Total and phosphorylated levels of ER α and the IGF-1 regulated signaling proteins MAPK and
360 AKT, were measured either 1- or 24-hours post-infusion.

361 *IGF-1-mediated phosphorylation of ER α in cytosolic compartment and subsequent increase in*
362 *total levels of ER α in the nuclear compartment require neuroestrogen synthesis.*

363 As a nuclear steroid receptor with the ability to be inserted into cell membranes, the
364 subcellular localization of ER α impacts the receptor's function. Therefore, we measured levels
365 of phosphorylated and total ER α levels in the cytosol, membrane, and nuclear compartments of
366 hippocampal cells at each time point.

367 In the cytosolic compartment (Figure 1), there was a main effect of treatment on levels of
368 pS118-ER α (F(2,27)=4.973; p=0.015) at 1 hour after treatment (Figure 1A), with levels of
369 pS118-ER α significantly increased in the IGF-1 treatment group as compared to the vehicle

370 group ($p=0.007$) and the IGF-1+Let treatment group ($p=0.020$). This observed increase in
371 phosphorylated ER α in the cytosol after 1 hour is consistent with earlier work in cell cultures
372 demonstrating that peak dimerization (and presumably therefore, nuclear translocation) of ER α
373 does not occur until two hours after estrogen treatment (Powell and Xu, 2008). However, there
374 was no significant difference in cytosolic pS118-ER α levels between the IGF-1+Let and vehicle
375 groups ($p=0.611$). There was no effect of treatment on total levels of cytosolic ER α 1-hour post-
376 infusion (Figure 1B; $F(2,27)=0.553$, $p=0.582$). At the 24-hour time point, there were no effects of
377 treatment on cytosolic levels of pS118-ER α (Figure 1C; $F(2,27)=0.292$, $p=0.750$) or total ER α
378 (Figure 1D; $F(2,27)=1.408$, $p=0.263$).

379 In the membrane compartment (Figure 2), there were no effects of treatment 1-hour
380 post-infusion on levels of pS118-ER α (Figure 2A, $F(2,25)=1.243$; $p=0.307$) or total ER α (Figure
381 2B, $F(2,27)=0.875$; $p=0.429$). There were also no effects of treatment 24-hours post-infusion on
382 membrane levels pS118-ER α (Figure 2C, $F(2,27)=2.122$; $p=0.141$) or total ER α (Figure 2D,
383 $F(2,27)=0.528$; $p=0.596$).

384 In the nuclear compartment (Figure 3), there were no effects of treatment on levels of
385 pS118-ER α (Figure 3A; $F(2,27)=0.095$, $p=0.910$) or total ER α (Figure 3B; $F(2,27)=0.202$,
386 $p=0.818$) 1-hour post-infusion. At the 24-hour timepoint, there was no effect of treatment on
387 pS118-ER α levels in the nuclear compartment (Figure 3C; $F(2,27)=0.084$, $p=0.919$). However,
388 there was an effect of treatment on total ER α levels in the nuclear compartment (Figure 3D;
389 $F(2,27)=3.915$, $p=0.033$) 24-hours post-infusion, with the IGF-1 treatment group showing
390 significantly higher levels as compared to the vehicle group ($p=0.011$) and near significantly
391 higher levels as compared to the IGF-1+Let group ($p=0.079$). There was no significant
392 difference in total ER α levels between the vehicle and IGF-1+Let treatment groups ($p=0.388$).

393 *In parallel to impacts of IGF-1 on ER α activation, IGF-1-mediated activation of MAPK, but not*
394 *Akt requires neuroestrogen synthesis.*

395 In order to determine if IGF-1 activation of ER α occurs via the MAPK or PI3K-Akt
396 signaling pathways and if IGF-1 activation of pathways require neuroestrogen synthesis, we
397 measured phosphorylated and total levels of p44-MAPK (ERK-1), p42-MAPK (ERK-2), and Akt.

398 One hour post infusion, there was a main effect of treatment on phosphorylation of both
399 p44 (Figure 4A; $F(2,27)= 35.750$, $p=4.65 \times 10^{-8}$) and p42 (Figure 4B; $F(2,27)= 21.720$,
400 $p=3.41 \times 10^{-6}$) phospho-sites of MAPK. Post hoc testing revealed a significant increase in
401 phosphorylation of both phospho-sites of MAPK in the IGF-1 treatment group as compared to
402 the Vehicle group (p44-MAPK, $p=2.39 \times 10^{-7}$; p42-MAPK, $p=2.59 \times 10^{-6}$) and the IGF-1 + Let
403 group (p44-MAPK, $p=5.20 \times 10^{-8}$; p42-MAPK, $p=1.48 \times 10^{-5}$). There was no difference between
404 the IGF-1 + Let group and the Veh group on phosphorylation of either p44 ($p=0.647$) or p42
405 ($p=0.407$) MAPK levels.

406 One hour post infusion, there was a main effect of treatment on phosphorylation of Akt
407 (Figure 4C; $F(2,27)= 7.552$, $p=0.003$). Post hoc testing revealed a significant increase in
408 phosphorylation of Akt in the IGF-1 group ($p=0.001$) and the IGF-1 + Let group ($p=0.006$) as
409 compared to the Veh group.

410 Twenty-four hours post infusion, there was no main effect of treatment on
411 phosphorylation of p44 MAPK (Figure 4D; $F(2,27)= 0.120$, $p=0.888$), p42 MAPK (Figure 4E;
412 $F(2,27)= 0.031$, $p=0.970$), or Akt (Figure 4F; $F(2,27)= 1.247$, $p=0.297$).

413

414 Experiment 2: Neuroestrogen synthesis is necessary for IGF-1-mediated enhancement of
415 spatial memory in recently ovariectomized middle-aged rats

416 Experiment 1 revealed that IGF-1 activation of the MAPK signaling pathway, associated
417 phosphorylation of ER α , and subsequent increase in levels of ER α in the hippocampus were
418 blocked by letrozole, suggesting that they require neuroestrogen synthesis. In Experiment 2, we

419 determined the functional consequences of these effects by testing the hypothesis that the
420 ability of IGF-1 to impact hippocampal-dependent memory in recently ovariectomized rats also
421 requires concomitant neuroestrogen synthesis. Additionally, we determined if IGF-1 activation of
422 signaling pathways in these behaviorally tested animals would parallel effects on memory.
423 Following training on the radial maze, recently ovariectomized middle-aged rats received
424 chronic icv treatment of either vehicle (Veh group), IGF-1 (IGF-1 group), or IGF-1 plus letrozole
425 (IGF-1 + Let group) and were tested on delay trials in the maze. Following maze testing,
426 hippocampal levels of MAPK and PI3K-Akt pathway activation were measured.

427 *IGF-1 enhances memory performance of recently ovariectomized rats on the radial-arm maze,*
428 *an enhancement that requires neuroestrogen synthesis.*

429 Following recovery from stereotaxic surgeries, animals were tested across multiple
430 increasing delays (1 hr, 3 hr, 4 hr, 5 hr) on the 8-arm radial maze test. As illustrated in Figure 5,
431 Mixed-Design ANOVA revealed a main effect of delay ($F(3,84)=4.257$; $p=0.008$) and a main
432 effect of treatment ($F(2,28)=5.245$; $p=0.012$) on radial-arm maze performance. Post hoc testing
433 revealed significantly fewer errors of 8 across delays in the IGF-1 group as compared to both
434 the Veh group ($p=0.004$) and the IGF-1 + Let group ($p=0.029$). There was no difference
435 between the Veh group and the IGF-1 + Let group. There was no significant interaction between
436 delay and treatment ($F(6,84)=1.555$; $p=0.171$).

437 *IGF-1 activation of MAPK, but not Akt signaling requires neuroestrogen synthesis in recently*
438 *ovariectomized, behaviorally tested rats*

439 Following chronic icv treatment with either IGF-1 or IGF-1 + Let, there was a main effect
440 of treatment on phosphorylation of p44-MAPK (Figure 6A; $F(2,30)=32.346$, $p=5.27 \times 10^{-7}$) and a
441 near significant effect of treatment on phosphorylation of p42-MAPK (Figure 6B; $F(2,30)=3.106$,
442 $p=0.060$). Post hoc testing revealed a significant increase in phosphorylation of p44-MAPK

443 levels in the IGF-1 group as compared to both the Veh group ($p=1.28 \times 10^{-7}$) and the IGF-1 + Let
444 group ($p=8.74 \times 10^{-8}$). There was also a significant increase in phosphorylation of p42-MAPK
445 levels in the IGF-1 group as compared to the Veh group ($p=0.020$) and a statistically trending
446 increase as compared to the IGF-1 + Let group ($p=0.104$). There was no difference between the
447 IGF-1 + Let group and the Veh group on phosphorylation of either p44 ($p=0.878$) or p42
448 ($p=0.418$) MAPK levels.

449 As illustrated in Figure 6C, there was a main effect of treatment on phosphorylation of
450 Akt ($F(2,30)= 4.803$, $p=0.016$). Post hoc testing revealed a significant increase in
451 phosphorylation of Akt in the IGF-1 group ($p=0.012$) and the IGF-1 + Let group ($p=0.013$) as
452 compared to the Veh group. There was no difference in levels of phosphorylation of Akt
453 between the IGF-1 and IGF-1 + Let groups ($p=0.907$).

454

455 Experiment 3: Long-term ovarian hormone deprivation disrupts interactions between IGF-1 and
456 neuroestrogen signaling resulting in detrimental impact of endogenous IGF-1 receptor activity
457 on memory.

458 Experiments 1 and 2 revealed that IGF-1-enhancement of hippocampal-dependent
459 memory and elevation of phosphorylated and total hippocampal levels of ER α in recently
460 ovariectomized rats requires concomitant neuroestrogen synthesis. Furthermore, results
461 suggest that these effects are mediated via activation of the MAPK and not the PI3K-Akt
462 signaling pathway. Previous evidence indicates that neuroestrogen synthesis is regulated by
463 circulating estrogens (Nelson et al 2016) and therefore, not surprisingly, long-term ovariectomy
464 results in decreased aromatase expression and neuroestrogen levels (Chen et al. 2021; Ma et
465 al 2020). In Experiment 3, we aimed to determine the implications of decreased level of
466 neuroestrogens resulting from long-term ovariectomy on IGF-1 signaling effects in the

467 hippocampus. We employed a rat model of menopause in which no post-ovariectomy estradiol
468 was administered, modeling women who do not use menopausal hormone therapy. Because we
469 aimed to assess effects of long-term loss of ovarian function on endogenous IGF-1 signaling
470 and subsequent impact for cognitive aging, we chose to antagonize IGF-1 here rather than
471 exogenously administer IGF-1 as was done in Experiments 1 and 2. Long-term ovariectomized
472 rats (100 days) that received no estradiol treatment received chronic icv delivery of vehicle (Veh
473 group) the IGF-1R antagonist JB1 (JB1 group), aromatase inhibitor letrozole (Let group), or JB1
474 plus letrozole (JB1+Let group) and were tested on the radial-maze task. Hippocampal levels of
475 MAPK and PI3K-Akt pathway activation were measured. Finally, hippocampal expression of
476 ER α , aromatase—the enzyme that converts testosterone to estradiol—and estradiol levels were
477 measured.

478 *Antagonizing IGF-1 receptor activity unexpectedly enhances spatial memory suggesting that*
479 *long-term ovariectomy leads to negative impacts of IGF-1 signaling on memory. Inhibition of*
480 *neuroestrogens reverses the enhancement, but has no impact on its own.*

481 As illustrated in Figure 7, Mixed-Design ANOVA revealed a main effect of delay
482 ($F(2,68)=6.713$; $p=0.002$) and a main effect of treatment ($F(3,34)=3.702$; $p=0.021$) on radial-arm
483 maze performance. Post hoc testing revealed significantly fewer errors of 8 across delays in the
484 JB1 group as compared to the Veh group ($p=0.012$). There was no difference between the Veh
485 group and the Let group ($p=0.417$) or between the Veh group and the JB1 + Let group
486 ($p=0.978$). There was no significant interaction between delay and treatment ($F(6,68)=0.419$;
487 $p=0.864$).

488 *Antagonizing IGF-1 receptor activity increases MAPK signaling and decreases Akt signaling*
489 *suggesting that under conditions of long-term ovarian hormone deprivation, PI3K-Akt signaling*
490 *pathway predominates. Inhibition of neuroestrogen synthesis reserves JB1-induced effects on*
491 *MAPK, but not on Akt.*

492 After chronic treatment with either JB1, letrozole, or JB1 plus letrozole following long-
493 term ovariectomy, there was an effect of treatment on phosphorylation of both p44-MAPK
494 (Figure 8A; $F(3,37)= 5.367$, $p=0.004$) and p42-MAPK (Figure 8B; $F(3,37)= 10.793$, $p=3.90 \times 10^{-5}$).
495 Post hoc testing revealed a significant increase in phosphorylation of p44-MAPK ($p=0.015$) and
496 p42-MAPK ($p=4.34 \times 10^{-4}$) levels in the JB1 group as compared to the Veh group. There were no
497 differences between the Veh group and the Let group for either p44-MAPK ($p=1.00$) or p42-
498 MAPK ($p=0.995$), nor were there any differences between the Veh group and the JB1+Let group
499 for either p44-MAPK ($p=0.805$) or p42-MAPK ($p=0.709$).

500 As illustrated in Figure 8C, there was an effect of treatment on phosphorylation of Akt
501 ($F(3,37)= 4.437$, $p=0.010$). Post hoc testing revealed a significant decrease in phosphorylation
502 of Akt in the JB1 group ($p=0.015$) and a near significant decrease in phosphorylation of Akt in
503 the JB1+Let group ($p=0.056$) as compared to the Veh group. There was no difference in levels
504 of phosphorylation of Akt between the Veh group and the Let group ($p=0.990$).

505 *Antagonism of IGF-1 receptors increases protein levels of ER α and aromatase in the*
506 *hippocampus, effects reversed by inhibition of neuroestrogen synthesis.*

507 As illustrated in Figure 9A, there was an effect of treatment on hippocampal ER α levels
508 ($F(3,37)= 4.202$, $p=0.012$). Post hoc testing revealed a significant increase in ER α expression in
509 the JB1 group ($p=0.011$) as compared to the Veh group. There was no difference in ER α levels
510 between the Veh group and the Let group ($p=0.940$) or between the Veh group and the JB1+Let
511 group ($p=0.997$).

512 There was a main effect of treatment on hippocampal aromatase levels, as shown in
513 Figure 9B ($F(3,37)= 6.65$, $p=0.001$). Post hoc testing revealed a significant increase in
514 aromatase expression in the JB1 group ($p=0.012$) as compared to the Veh group. There was no

515 difference in aromatase levels between the Veh group and the Let group ($p=0.974$) or between
516 the Veh group and the JB1+Let group ($p=0.403$).

517 *Neither antagonism of IGF-1 receptors nor inhibition of neuroestrogen synthesis*
518 *impacted levels of locally synthesized neuroestrogens. The lack of effect of letrozole on*
519 *estradiol levels suggests low baseline levels of locally synthesized neuroestrogens in the*
520 *hippocampus following long-term ovariectomy.*

521 After chronic treatment with either JB1, letrozole, or JB1 plus letrozole following long-term
522 ovariectomy, there was no effect of treatment on hippocampal estradiol levels (Figure 10A;
523 $F(3,29)= 0.466$, $p=0.708$).

524

525 Experiment 4: A history of previous midlife estradiol treatment protects hippocampal function
526 and memory following long-term ovarian hormone deprivation by maintaining the interactive
527 relationship between IGF-1 and neuroestrogen signaling.

528 Results of Experiment 3 revealed that long-term ovarian deprivation disrupts the ability
529 of IGF-1 and neuroestrogens to exert positive interactive effects on memory as indicated by an
530 enhancement resulting from IGF-1 receptor antagonism and a lack of disruptive effects on
531 memory of letrozole treatment alone. In contrast to the Experiment 3 results in which JB1
532 enhanced memory, previous work from our lab revealed that antagonism of IGF-1 receptors by
533 JB1 disrupts memory in ovariectomized rats treated with ongoing (Nelson et al. 2014) or
534 previous (Witty et al. 2013) estradiol. In Experiment 4, we tested the hypothesis that previous
535 midlife estradiol exposure maintains the positive impact of IGF-1 signaling on the MAPK
536 signaling pathway, ER α levels and subsequent impact on memory by sustaining neuroestrogen
537 synthesis in the hippocampus long-term, even after termination of estradiol treatment and in the
538 absence of circulating estrogens. We employed a rat model of menopause in which middle-

539 aged animals received an estradiol implant at the time of ovariectomy that was removed
540 following 40 days of treatment, modeling women who take hormones for a few years and then
541 stop. One hundred days following termination of estradiol treatment, rats were treated with
542 chronic icv delivery of vehicle (Veh group), IGF-1R antagonist JB1 (JB1 group), aromatase
543 inhibitor letrozole (Let group), or JB1 plus letrozole (JB1+Let group). Rats were then tested on a
544 hippocampal-dependent spatial memory task and later hippocampal levels of MAPK and PI3K-
545 Akt pathway activation, ER α and aromatase expression, and estradiol levels were measured.
546 *Antagonizing IGF-1 receptor activity, inhibition of neuroestrogen synthesis, or the combination*
547 *of both exert similar detrimental effects on spatial memory. Results indicate that a previous*
548 *history of estradiol treatment allows for long-term maintenance of the beneficial interactive*
549 *effects of IGF-1 and neuroestrogens in the hippocampus, in which both are necessary, but*
550 *neither sufficient to enhance memory.*

551 As illustrated in 7, Mixed-Design ANOVA revealed a main effect of delay
552 ($F(4,124)=20.720$; $p=4.26 \times 10^{-13}$) and a main effect of treatment ($F(3,31)=3.205$; $p=0.037$) on
553 radial-arm maze performance. Post hoc testing revealed significantly more errors of 8 across
554 delays in the JB1 group ($p=0.033$), the Let group ($p=0.033$), and the JB1+Let group ($p=0.012$)
555 as compared to the Veh group. There was a statistically trending interaction between delay and
556 treatment ($F(12, 124)=1.655$; $p=0.085$).

557 *Antagonizing IGF-1 receptor activity, inhibition of neuroestrogen synthesis, or the*
558 *combination of both, resulted in similar decreased levels of MAPK activation, and no effects of*
559 *on Akt activation. Results indicate that after a previous history of estradiol treatment, MAPK*
560 *signaling pathway predominates due to interactions of IGF-1 and neuroestrogen signaling.*

561 After chronic treatment with either JB1, letrozole, or JB1 plus letrozole following
562 previous estradiol exposure, there was an effect of treatment on phosphorylation of both p44-

563 MAPK (Figure 8D; $F(3,34)= 3.694$, $p=0.022$) and p42-MAPK (Figure 8E; $F(3,34)= 4.839$,
564 $p=0.007$). Post hoc testing revealed a significant decrease in phosphorylation of both
565 phosphorylation sites of MAPK in the JB1 group (p44-MAPK, $p=0.022$; p42-MAPK, $p=0.008$),
566 the Let group (p44-MAPK, $p=0.035$; p42-MAPK, $p=0.007$), and the JB1+Let group (p44-MAPK,
567 $p=0.034$; p42-MAPK, $p=0.038$) as compared to the Veh group.

568 As illustrated in Figure 8F, there was an effect of treatment on phosphorylation of Akt
569 ($F(3,34)= 3.248$, $p=0.035$). However, post hoc testing revealed no significant differences
570 between the Veh group and the JB1 ($p=0.363$), Let ($p=0.350$), or JB1+Let ($p=0.615$) groups.

571 *Antagonizing IGF-1 receptor activity, inhibition of neuroestrogen synthesis, or the*
572 *combination of both results in similar decreases in protein levels of ER α and aromatase in the*
573 *hippocampus.*

574 As illustrated in Figure 9C, there was an effect of treatment on hippocampal ER α levels
575 ($F(3,34)= 4.008$, $p=0.016$). Post hoc testing revealed a significant decrease in ER α expression
576 in the JB1 group ($p=0.034$), the Let group ($p=0.023$), and the JB1+Let group ($p=0.016$) as
577 compared to the Veh group.

578 Finally, there was an effect of treatment on hippocampal aromatase levels, as shown in
579 Figure 9D ($F(3,34)= 8.803$, $p=2.27 \times 10^{-4}$). Post hoc testing revealed a significant decrease in
580 aromatase expression in the JB1 group ($p=0.009$), the Let group ($p=4.43 \times 10^{-4}$), and the JB1+Let
581 group ($p=2.26 \times 10^{-4}$) as compared to the Veh group.

582 *Antagonizing IGF-1 receptor activity, inhibition of neuroestrogen synthesis, or the*
583 *combination of both results in similar decreased levels of locally synthesized neuroestrogens.*
584 *The effect of letrozole on estradiol levels suggests that local synthesis of neuroestrogens in the*
585 *hippocampus is maintained by a history of previous midlife estradiol treatment following long-*
586 *term ovariectomy.*

587 After chronic treatment with either JB1, letrozole, or JB1 plus letrozole following previous
588 estradiol exposure, there was an effect of treatment on hippocampal estradiol levels (Figure
589 10B; $F(3,29)=3.10$, $p=0.044$). Post hoc testing revealed a significant decrease in estradiol
590 expression in the JB1 group ($p=0.024$), the Let group ($p=0.027$), and the JB1+Let group
591 ($p=0.048$) as compared to the Veh group.

592

593

594 **Discussion**

595 Results reveal that short-term estrogen treatment during midlife—as is commonly used
596 during the menopausal transition in humans—provides lasting benefits for hippocampal function
597 and memory by robustly altering the interactive relationship between insulin-like growth factor-1
598 (IGF-1) and locally synthesized neuroestrogens in mediating ligand-independent activation of
599 hippocampal estrogen receptor (ER) α . First, we showed in recently ovariectomized rats (~10-
600 day) that neuroestrogen synthesis is required for IGF-1-mediated increases in phosphorylation
601 of ER α , activation of the MAPK pathway, and enhanced performance on the hippocampal-
602 dependent radial-arm maze. Next, we found that following long-term ovariectomy (~100-day),
603 IGF-1 signaling and neuroestrogen signaling no longer provided the same benefits for
604 hippocampal function and memory, demonstrating a weakened relationship between the two
605 hormones following long periods of ovarian hormone deprivation. Remarkably, short-term (40-
606 day) treatment with estradiol immediately following ovariectomy successfully maintained the
607 relationship between IGF-1 and neuroestrogen signaling, resulting in enhanced memory,
608 increased hippocampal activation of MAPK, protein expression of ER α and aromatase, and
609 estradiol levels. Together, results provide a potential model for combatting postmenopausal
610 cognitive decline in which short-term estradiol treatment near the loss of ovarian hormones can
611 sustain hippocampal function and memory by maintaining the dynamic relationships between
612 ER α , IGF-1R, and neuroestrogen synthesis in the aging female brain.

613

614 Effects of IGF-1 on ER α activation, MAPK signaling and memory rely on local estrogen
615 production.

616

617 Results of Experiment 1 revealed that infusion of IGF-1 to brains of ovariectomized rats
618 increased phosphorylation of hippocampal ER α at S118—a site associated with decreased
619 degradation (Valley et al. 2005) and increased transcriptional activity (Duterte and Smith, 2003)
620 of the receptor. Subcellular compartment fractionation allowed us to localize the increased
621 pS118-ER α that occurred one hour following IGF-1 infusion to the cytosolic compartment of
622 hippocampal cells. Results are consistent with *in vitro* work demonstrating peak dimerization
623 (and presumably therefore, nuclear translocation) of ER α does not occur until two hours after
624 estrogen treatment (Powell and Xu, 2008). Twenty-four hours after infusion of IGF-1, overall
625 ER α levels were increased in the nuclear compartment of hippocampal cells. Results suggest
626 that IGF-1 activation of ER α via phosphorylation at S118 promotes nuclear translocation of
627 ER α , protecting the receptor from degradation and allowing for sustained ER α levels.
628 Furthermore, results implicate a role for locally synthesized neuroestrogens in IGF-1 effects.
629 Inhibition of local synthesis of neuroestrogens via administration of letrozole blocked the ability
630 of IGF-1 to increase phosphorylation of ER α and the subsequent increase in nuclear ER α
631 protein levels.

632 A potential mechanism by which IGF-1 and neuroestrogen interact to impact ER α is via
633 intracellular signaling pathways. Both MAPK and PI3K-Akt signaling are activated via tyrosine
634 kinase receptor IGF-1 or by neuroestrogens acting on membrane-bound estrogen receptors
635 (Russo et al. 2005; Foster 2012). Here, infusions of IGF-1, but not IGF-1 plus letrozole, increase
636 phosphorylation of p44- and p42-MAPK. Letrozole had no impact on IGF-1-induced increase in
637 Akt phosphorylation. Earlier work in cell culture demonstrated that MAPK phosphorylates ER α
638 at S118 following IGF-1 treatment (Kato et al. 1995), and recent *in vitro* work from our lab
639 support the role of neuroestrogens in activating the MAPK pathway in conjunction with IGF-1R
640 (Pollard and Daniel, 2019). Interestingly, Pollard and Daniel (2019) also demonstrated a
641 mutually repressive relationship between MAPK and Akt in which both pathways inhibit each

642 other, allowing for highly regulated control of ER α activity by IGF-1R. In summary, data indicate
643 that IGF-1 and neuroestrogen signaling interact via the MAPK, but not the Akt, pathway, to
644 activate hippocampal ER α in the absence of circulating estrogens. The significance of these
645 interactions is supported by the results of Experiment 2 in which IGF-1 mediated enhancement
646 of a hippocampal dependent radial-maze task was blocked by letrozole, indicating that IGF-1
647 activation of ER α requires neuroestrogen synthesis to enhance hippocampal memory.

648

649 Effects of IGF-1 on MAPK signaling and memory are significantly altered as a result of long-
650 term loss of ovarian function and associated putative decrease in neuroestrogens.

651 Local inhibition of aromatase activity has been shown to impair memory consolidation in
652 recently ovariectomized mice (Tuscher et al 2016). However, hippocampal aromatase
653 expression (Ma et al 2020), estradiol levels (Chen et al 2021), and neuroestrogen-mediated
654 transcriptional activity (Baumgartner et al 2019) decrease following long-term, but not short-
655 term, ovariectomy. Consistent with those findings are results of Experiment 3 in which blocking
656 neuroestrogen synthesis via letrozole administration had no impact on hippocampal memory in
657 long-term ovariectomized animals. Surprisingly, pharmacologically inhibiting IGF-1R using JB1
658 actually enhanced memory in long-term ovariectomized rats, suggesting the possibility that IGF-
659 1 signaling becomes detrimental following long-term ovarian hormone deprivation and
660 associated loss of local synthesis of neuroestrogens.

661 The paradoxical beneficial effect of IGF-1 antagonism on memory following long-term
662 ovarian hormone deprivation could potentially be explained by regulation of aromatase activity
663 via IGF-1 signaling. In addition to enhancement of memory, blocking IGF-1R with JB1 in long-
664 term ovariectomized animals resulted in increased hippocampal MAPK activation, decreased
665 PI3K-Akt activation, and increased expression of ER α and aromatase. Importantly, JB1 plus

666 letrozole did not have the same effects on memory and protein expression as JB1 administered
667 alone, indicating that the positive impacts of JB1 on memory require subsequent
668 neuroestrogens synthesis. While the precise mechanism for activation of the enzyme aromatase
669 is far from clear—with certain phospho-sites associated with increased activity, and others
670 associated with suppressed activity (Balthazart et al. 2005; Catalano et al. 2009; Miller et al.
671 2008)—its activation can be regulated by kinase cascades initiated by IGF-1R and membrane
672 estrogen receptors. For example, in T47D breast cancer cells, inhibition of the Akt pathway was
673 associated with increased aromatase activity (Su et al 2011). Here, results suggest a
674 mechanism in which inhibiting IGF-1R results in decreased PI3K-Akt activation, which in turn
675 disinhibits the MAPK pathway and allows for increased ER α and aromatase. Ultimately,
676 however, we detected no group differences in hippocampal estradiol levels following long-term
677 ovariectomy, likely due to overall decreases in estradiol levels following long periods of ovarian
678 hormone deprivation reported previously (Chen et al 2021). Nevertheless, results suggest that a
679 shift in IGF-1 signaling from MAPK to PI3K-Akt following long-term ovarian hormone deprivation
680 is detrimental to memory.

681

682 Effects of long-term loss of ovarian function are mitigated by early, short-term estrogen
683 treatment, and reflect effects on levels of aromatase and neuroestrogens.

684 Results of Experiment 4 demonstrate that a history of previous estradiol treatment
685 reverses the negative effects of IGF-1 signaling on the hippocampus and memory in long-term
686 ovariectomized rats. Consistent with earlier work (Witty et al. 2013), we found that JB1
687 treatment impaired memory and decreased levels of MAPK phosphorylation and ER α
688 expression in animals previously treated with estradiol during midlife. Here we extend those
689 findings by demonstrating the necessary role for neuroestrogens in facilitating activation of the
690 MAPK pathway by IGF-1R. We found identical effects of JB1, letrozole, and JB1 plus letrozole

691 on memory, MAPK phosphorylation, ER α and aromatase protein expression, and hippocampal
692 estradiol levels in animals that experienced previous estradiol treatment, indicating that IGF-1R
693 and neuroestrogens work together to maintain hippocampal function in aging females following
694 a previous period of midlife estradiol treatment.

695 The current results reveal diverging paths for hippocampal function in two models of
696 menopause. On one path, long-term loss of ovarian hormones results in decreased
697 neuroestrogen activity, shifting the balance of IGF-1 signaling such that activation of the Akt
698 pathway predominates over activation of the MAPK pathway, and leading to decreases in levels
699 of aromatase and phosphorylation of ER α . On the other path, a short-term period of estradiol
700 treatment immediately following loss of ovarian function reverses the negative impact of long-
701 term hormone deprivation on hippocampal function by sustaining levels of neuroestrogens well
702 beyond the period of estradiol treatment, allowing for IGF-1 mediated activation of the MAPK
703 pathway to predominate over the Akt pathway. MAPK signaling leads to increased aromatase
704 expression, continued neuroestrogens synthesis, and phosphorylation of ER α at phospho-site
705 Ser-118. This activation via ligand-independent mechanisms results in dimerization and nuclear
706 translocation of ER α , allowing for sustained levels of the receptor and leading to transcriptional
707 changes that impact hippocampal function and ultimately enhance memory.

708 **CONCLUSIONS**

709 Collectively, results indicate that short-term estrogen treatment following midlife loss of ovarian
710 function has long-lasting effects on hippocampal function and memory by dynamically regulating
711 cellular mechanisms that promote activity of ER α in the absence of circulating estrogens.
712 Findings demonstrate how changes in hippocampal ER α expression, IGF-1R signaling, and
713 neuroestrogen synthesis following long-term ovariectomy can negatively impact memory, but
714 that a history of previous estradiol treatment protects the hippocampus against these changes
715 to combat cognitive decline in rodent models of menopause.

716 References

717 Balthazart J, Baillien M, Ball G. Interactions Between Kinases and Phosphatases in the Rapid
718 Control of Brain Aromatase. *J Neuroendocrinol.* 2005 Sep;17(9), 553-559. doi: 10.1111/j.1365-
719 2826.2005.01344.x

720 Baumgartner NE, Black KL, McQuillen SM, Daniel JM. (2021). Previous estradiol treatment
721 during midlife maintains transcriptional regulation of memory-related proteins by ER α in the
722 hippocampus in a rat model of menopause. *Neurobiol Aging.* 2021 Sep;105:365-373. doi:
723 10.1016/j.neurobiolaging.2021.05.022. Epub 2021 Jun 5. PMID: 34198140; PMCID:
724 PMC8338908.

725 Baumgartner NE, Daniel JM. Estrogen receptor α : a critical role in successful female cognitive
726 aging. *Climacteric.* 2021 Aug;24(4):333-339. doi: 10.1080/13697137.2021.1875426. Epub 2021
727 Feb 1. PMID: 33522313; PMCID: PMC8273070.

728 Baumgartner NE, Grissom EM, Pollard KJ, McQuillen SM, Daniel JM. Neuroestrogen-
729 Dependent Transcriptional Activity in the Brains of ERE-Luciferase Reporter Mice following
730 Short- and Long-Term Ovariectomy. *eNeuro.* 2019 Oct 16;6(5):ENEURO.0275-19.2019. doi:
731 10.1523/ENEURO.0275-19.2019. PMID: 31575604; PMCID: PMC6795557.

732 Black KL, Witty CF, Daniel JM. Previous Midlife Oestradiol Treatment Results in Long-Term
733 Maintenance of Hippocampal Oestrogen Receptor α Levels in Ovariectomised Rats:
734 Mechanisms and Implications for Memory. *J Neuroendocrinol.* 2016
735 Oct;28(10):10.1111/jne.12429. doi: 10.1111/jne.12429. PMID: 27603028; PMCID:
736 PMC5527336.

737 Cardona-Gómez GP, DonCarlos L, Garcia-Segura LM. Insulin-like growth factor I receptors and
738 estrogen receptors colocalize in female rat brain. *Neuroscience.* 2000;99(4):751-60. doi:
739 10.1016/s0306-4522(00)00228-1. PMID: 10974438.

- 740 Catalano S, Barone I, Giordano C, Rizza P, Qi H, Gu G, Malivindi R, Bonofiglio D, Andò S.
741 Rapid estradiol/ERalpha signaling enhances aromatase enzymatic activity in breast cancer
742 cells. *Mol Endocrinol*. 2009 Oct;23(10), 1634-1645. doi: 10.1210/me.2009-0039
- 743 Chen HB, Xu C, Zhou MH, Qiao H, An SC. Endogenous hippocampal, not peripheral, estradiol
744 is the key factor affecting the novel object recognition abilities of female rats. *Behav Neurosci*.
745 2021 Oct;135(5):668-679. doi: 10.1037/bne0000480. Epub 2021 Aug 16. PMID: 34398621.
- 746 Daniel J.M. (2015) The Land Radial-Arm Maze: Eight Out of Eight Arms Baited with Food
747 Protocol for Rodents. In: Bimonte-Nelson H. (eds) *The Maze Book*. *Neuromethods*, vol 94.
748 Humana Press, New York, NY. https://doi.org/10.1007/978-1-4939-2159-1_17
- 749 Dutertre M, Smith CL. Ligand-independent interactions of p160/steroid receptor coactivators
750 and CREB-binding protein (CBP) with estrogen receptor-alpha: regulation by phosphorylation
751 sites in the A/B region depends on other receptor domains. *Mol Endocrinol*. 2003
752 Jul;17(7):1296-314. doi: 10.1210/me.2001-0316. Epub 2003 Apr 24. PMID: 12714702.
- 753 Foster TC. Role of estrogen receptor alpha and beta expression and signaling on cognitive
754 function during aging. *Hippocampus*. 2012 Apr;22(4):656-69. doi: 10.1002/hipo.20935. Epub
755 2011 Apr 27. PMID: 21538657; PMCID: PMC3704216.
- 756 Grissom EM, Daniel JM. Evidence for Ligand-Independent Activation of Hippocampal Estrogen
757 Receptor- α by IGF-1 in Hippocampus of Ovariectomized Rats. *Endocrinology*. 2016
758 Aug;157(8):3149-56. doi: 10.1210/en.2016-1197. Epub 2016 Jun 2. PMID: 27254005; PMCID:
759 PMC4967122.
- 760 Henderson VW, Watt L, Buckwalter JG. Cognitive skills associated with estrogen replacement in
761 women with Alzheimer's disease. *Psychoneuroendocrinology*. 1996 May;21(4):421-30. doi:
762 10.1016/0306-4530(95)00060-7. PMID: 8844880.

- 763 Kato S, Endoh H, Masuhiro Y, Kitamoto T, Uchiyama S, Sasaki H, Masushige S, Gotoh Y,
764 Nishida E, Kawashima H, Metzger D, Chambon P. Activation of the estrogen receptor through
765 phosphorylation by mitogen-activated protein kinase. *Science*. 1995 Dec 1;270(5241):1491-4.
766 doi: 10.1126/science.270.5241.1491. PMID: 7491495.
- 767 Li J, Gibbs RB. Detection of estradiol in rat brain tissues: Contribution of local versus systemic
768 production. *Psychoneuroendocrinology*. 2019 Apr;102:84-94. doi:
769 10.1016/j.psyneuen.2018.11.037. Epub 2018 Dec 1. PMID: 30529907.
- 770 Li J, Oberly PJ, Poloyac SM, Gibbs RB. A microsomal based method to detect aromatase
771 activity in different brain regions of the rat using ultra performance liquid chromatography-mass
772 spectrometry. *J Steroid Biochem Mol Biol*. 2016 Oct;163:113-20. doi:
773 10.1016/j.jsbmb.2016.04.013. Epub 2016 Apr 22. PMID: 27113434.
- 774 Ma Y, Liu M, Yang L, Zhang L, Guo H, Hou W, Qin P. Loss of Estrogen Efficacy Against
775 Hippocampus Damage in Long-Term OVX Mice Is Related to the Reduction of Hippocampus
776 Local Estrogen Production and Estrogen Receptor Degradation. *Mol Neurobiol*. 2020
777 Aug;57(8):3540-3551. doi: 10.1007/s12035-020-01960-z. Epub 2020 Jun 15. PMID: 32542593.
- 778 Mendez P, Azcoitia I, Garcia-Segura LM. Estrogen receptor alpha forms estrogen-dependent
779 multimolecular complexes with insulin-like growth factor receptor and phosphatidylinositol 3-
780 kinase in the adult rat brain. *Brain Res Mol Brain Res*. 2003 Apr 10;112(1-2):170-6. doi:
781 10.1016/s0169-328x(03)00088-3. PMID: 12670715.
- 782 Miller TW, Shin I, Kagawa N, Evans DB, Waterman MR, Arteaga CL. Aromatase is
783 phosphorylated in situ at Serine-118. *J Steroid Biochem Mol Biol*. 2008 Nov;112(1-3), 95-101.
784 doi: 10.1016/j.jsbmb.2008.09.001
- 785 Nelson BS, Black KL, Daniel JM. Circulating Estradiol Regulates Brain-Derived Estradiol via
786 Actions at GnRH Receptors to Impact Memory in Ovariectomized Rats. *eNeuro*. 2016 Dec

787 13;3(6):ENEURO.0321-16.2016. doi: 10.1523/ENEURO.0321-16.2016. PMID: 28032117;

788 PMCID: PMC5172373.

789 Nelson BS, Springer RC, Daniel JM. Antagonism of brain insulin-like growth factor-1 receptors

790 blocks estradiol effects on memory and levels of hippocampal synaptic proteins in

791 ovariectomized rats. *Psychopharmacology*. 2014 Mar; 231(5):899-907. doi: 10.1007/s00213-

792 013-3310-7. PMID: 24146138.

793 Pollard KJ, Daniel JM. Nuclear estrogen receptor activation by insulin-like growth factor-1 in

794 Neuro-2A neuroblastoma cells requires endogenous estrogen synthesis and is mediated by

795 mutually repressive MAPK and PI3K cascades. *Mol Cell Endocrinol*. 2019 Jun 15;490:68-79.

796 doi: 10.1016/j.mce.2019.04.007. Epub 2019 Apr 13. PMID: 30986444; PMCID: PMC6520186.

797 Pollard KJ, Wartman HD, Daniel JM. Previous estradiol treatment in ovariectomized mice

798 provides lasting enhancement of memory and brain estrogen receptor activity. *Horm Behav*.

799 2018 Jun;102:76-84. doi: 10.1016/j.yhbeh.2018.05.002. Epub 2018 May 12. PMID: 29742445;

800 PMCID: PMC6004337.

801 Powell E, Wang Y, Shapiro DJ, Xu W. Differential requirements of Hsp90 and DNA for the

802 formation of estrogen receptor homodimers and heterodimers. *J Biol Chem*. 2010 May

803 21;285(21):16125-34. doi: 10.1074/jbc.M110.104356. Epub 2010 Mar 30. PMID: 20353944;

804 PMCID: PMC2871481.

805 Rodgers SP, Bohacek J, Daniel JM. Transient estradiol exposure during middle age in

806 ovariectomized rats exerts lasting effects on cognitive function and the hippocampus.

807 *Endocrinology*. 2010 Mar;151(3):1194-203. doi: 10.1210/en.2009-1245. Epub 2010 Jan 12.

808 PMID: 20068005.

809 Russo VC, Gluckman PD, Feldman EL, Werther GA. The insulin-like growth factor system and
810 its pleiotropic functions in brain. *Endocr Rev.* 2005 Dec;26(7):916-43. doi: 10.1210/er.2004-
811 0024. Epub 2005 Aug 30. PMID: 16131630.

812 Sherwin BB. Estrogenic effects on memory in women. *Ann N Y Acad Sci.* 1994 Nov 14;743:213-
813 30; discussion 230-1. doi: 10.1111/j.1749-6632.1994.tb55794.x. PMID: 7802415.

814 Sohrabji F. Estrogen-IGF-1 interactions in neuroprotection: ischemic stroke as a case study.
815 *Front Neuroendocrinol.* 2015 Jan;36:1-14. doi: 10.1016/j.yfrne.2014.05.003.

816 Su B, Wong C, Hong Y, Chen S. Growth factor signaling enhances aromatase activity of breast
817 cancer cells via post-transcriptional mechanisms. *J Steroid Biochem Mol Biol.* 2011 Feb;123(3-
818 5), 101-108. doi: 10.1016/j.jsbmb.2010.11.012

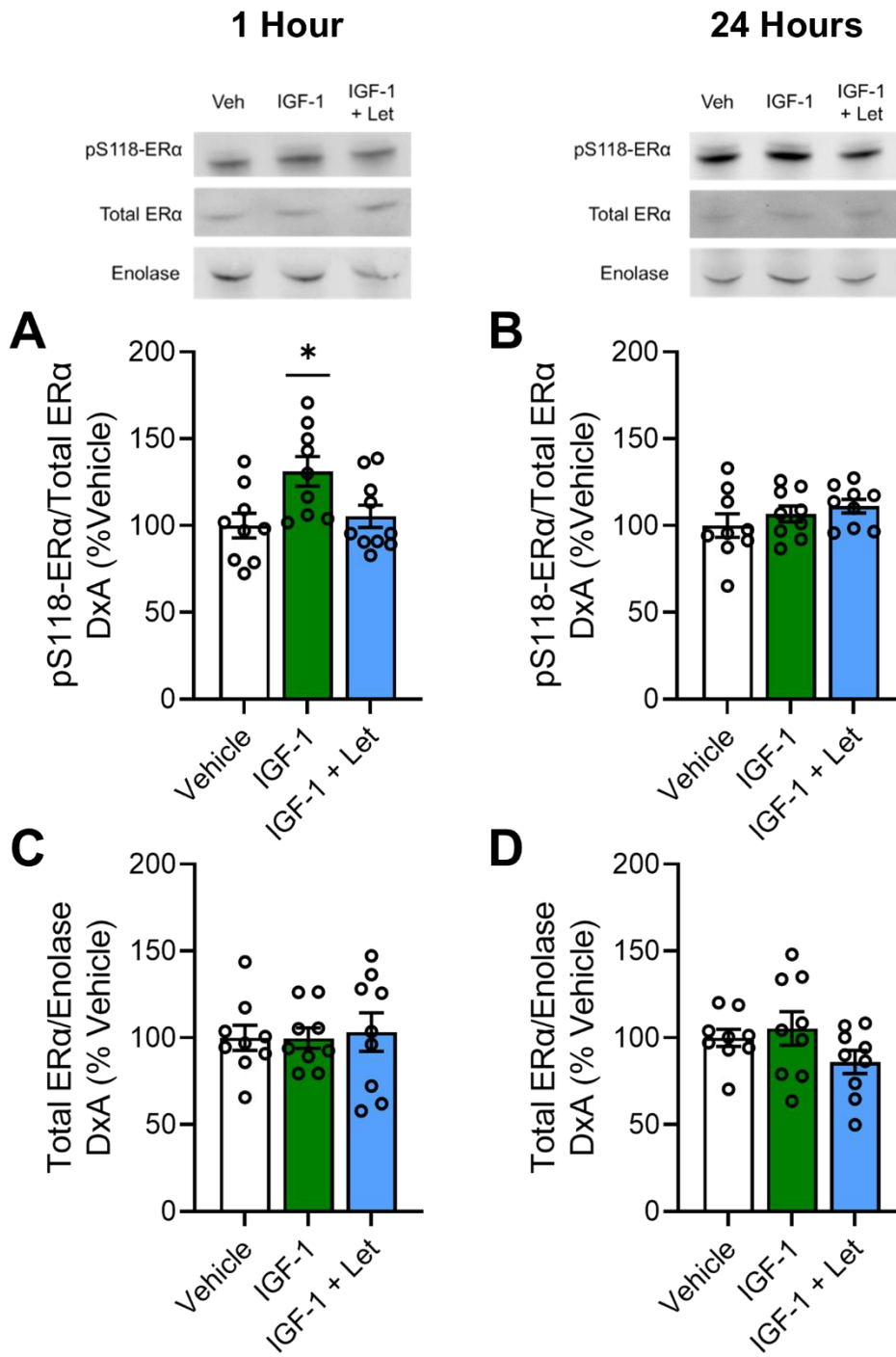
819 Tuscher JJ, Szinte JS, Starrett JR, Krentzel AA, Fortress AM, Remage-Healey L, Frick KM.
820 Inhibition of local estrogen synthesis in the hippocampus impairs hippocampal memory
821 consolidation in ovariectomized female mice. *Horm Behav.* 2016 Jul;83, 60-67. doi:
822 10.1016/j.yhbeh.2016.05.001

823 Valley CC, Métivier R, Solodin NM, Fowler AM, Mashek MT, Hill L, Alarid ET. Differential
824 regulation of estrogen-inducible proteolysis and transcription by the estrogen receptor alpha N
825 terminus. *Mol Cell Biol.* 2005 Jul;25(13):5417-28. doi: 10.1128/MCB.25.13.5417-5428.2005.
826 PMID: 15964799; PMCID: PMC1156995.

827 Witty CF, Gardella LP, Perez MC, Daniel JM. Short-term estradiol administration in aging
828 ovariectomized rats provides lasting benefits for memory and the hippocampus: a role for
829 insulin-like growth factor-I. *Endocrinology.* 2013 Feb;154(2):842-52. doi: 10.1210/en.2012-1698.
830 Epub 2012 Dec 21. PMID: 23264616.

831

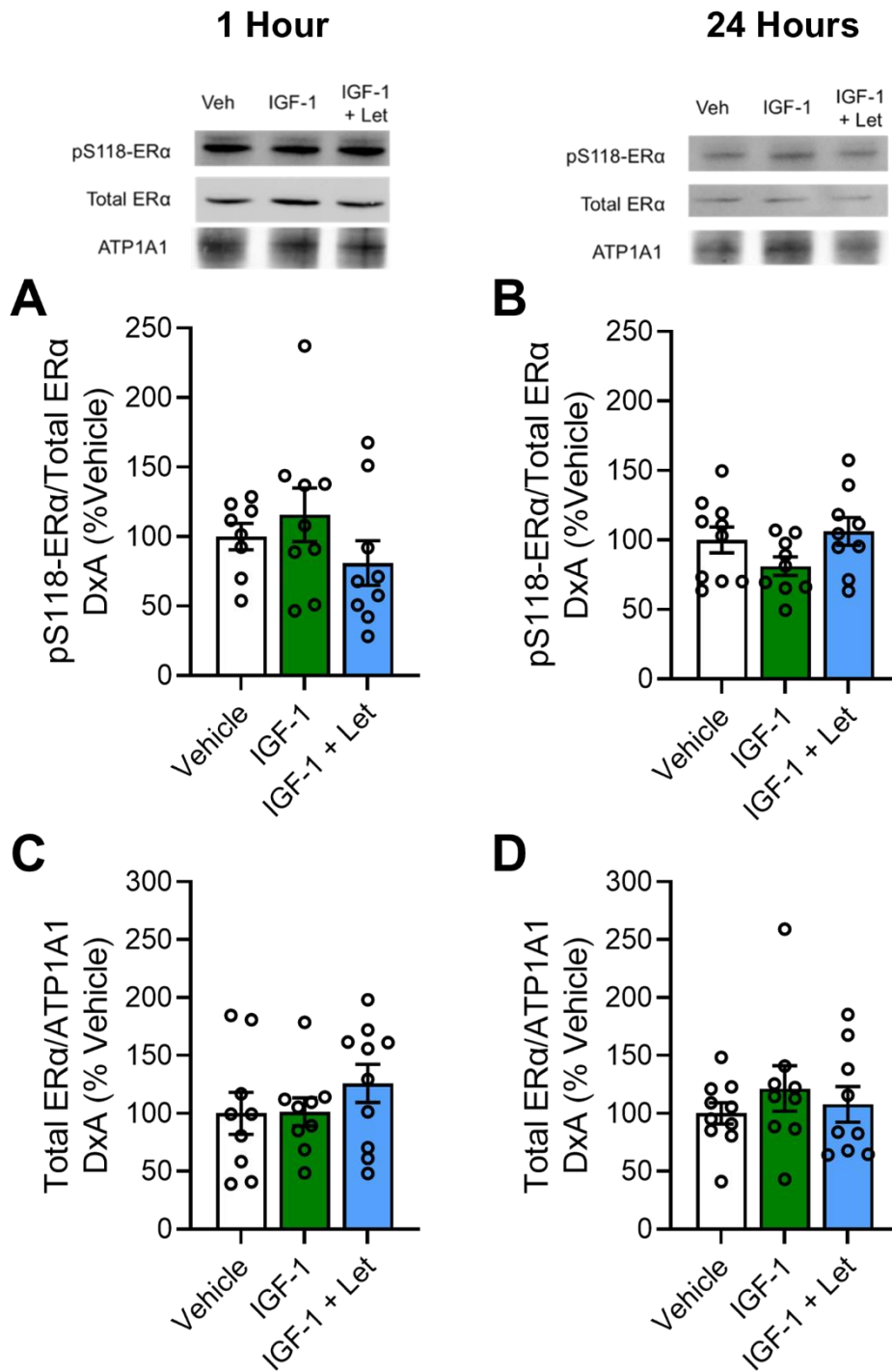
832 Figure 1



833

834

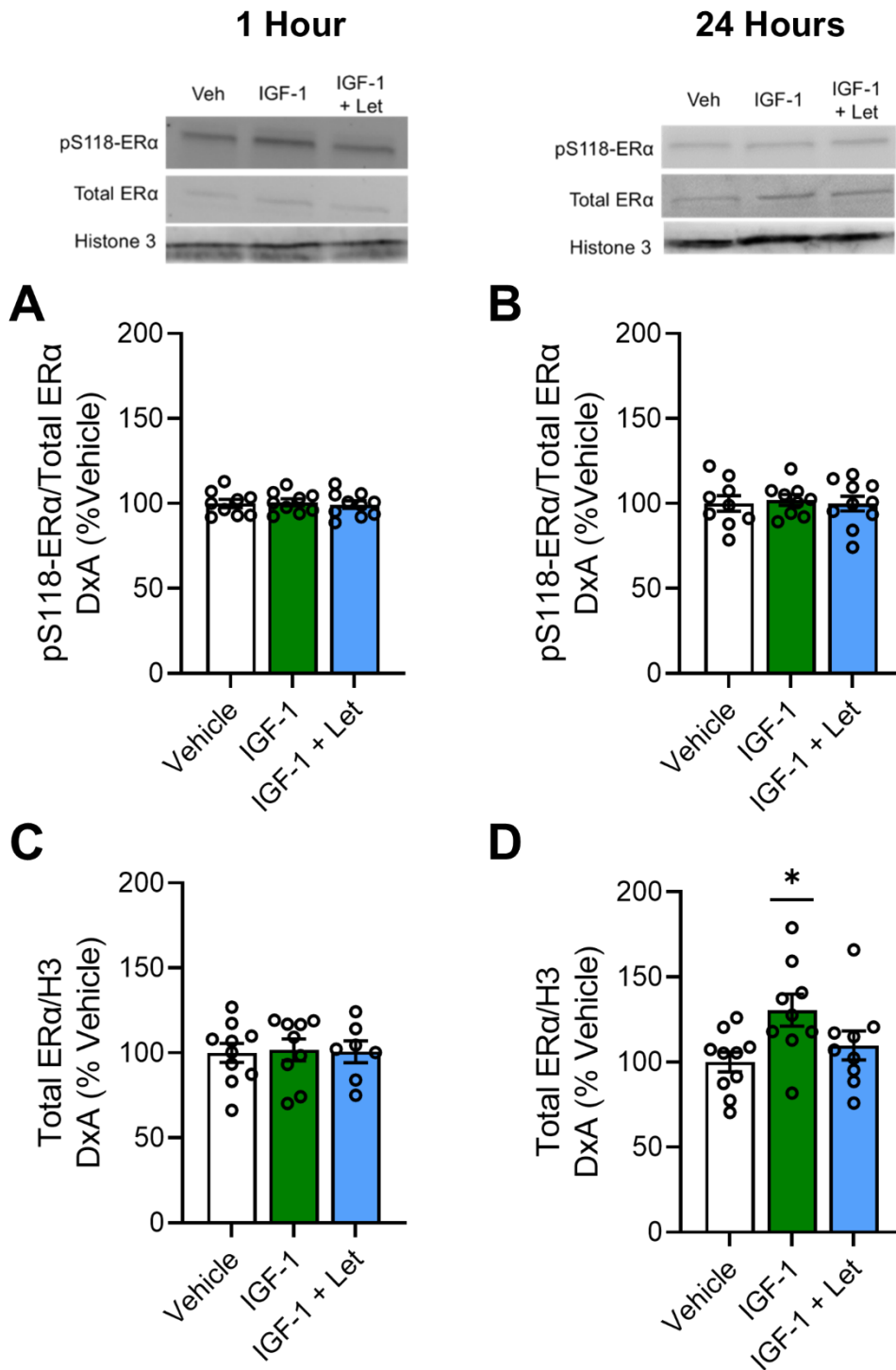
835 Figure 2



836

837

838 Figure 3



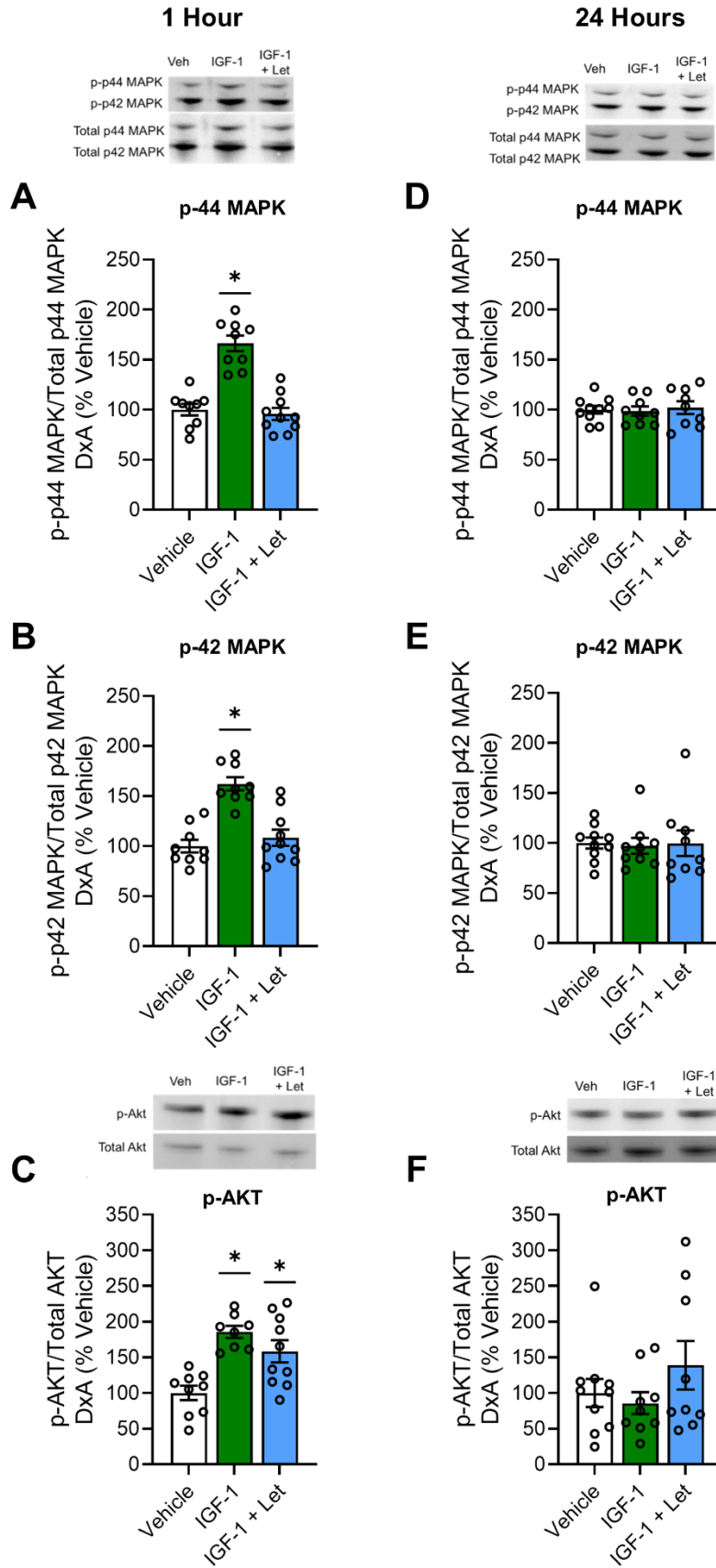
839

840

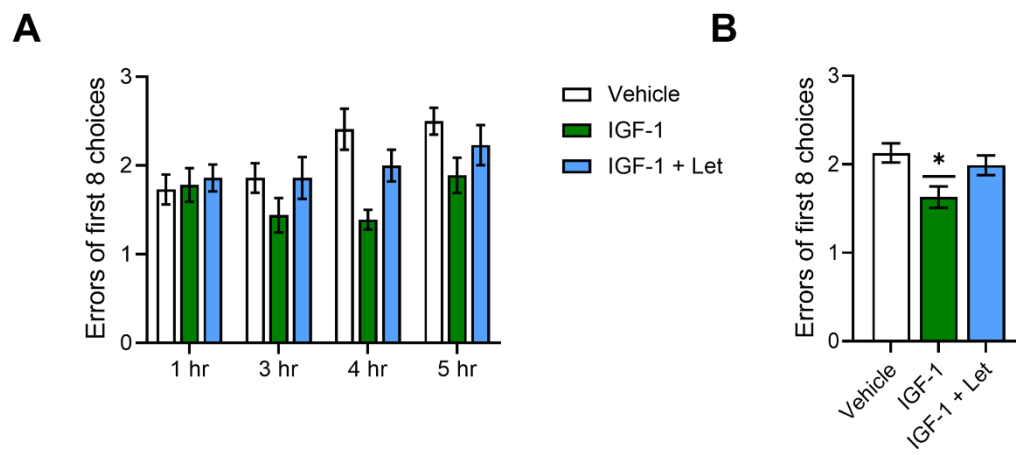
841 Figure 4

842

843



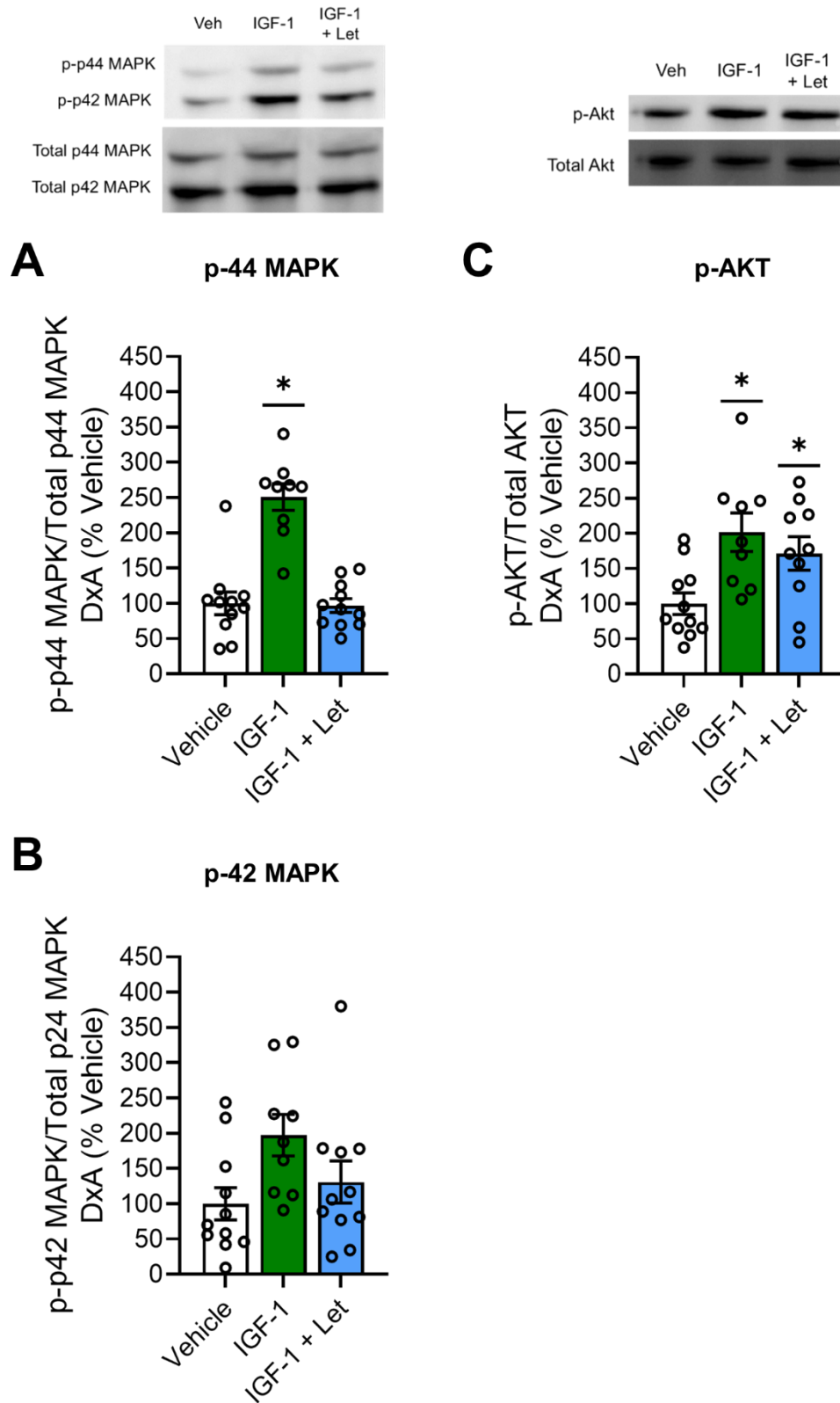
844 Figure 5



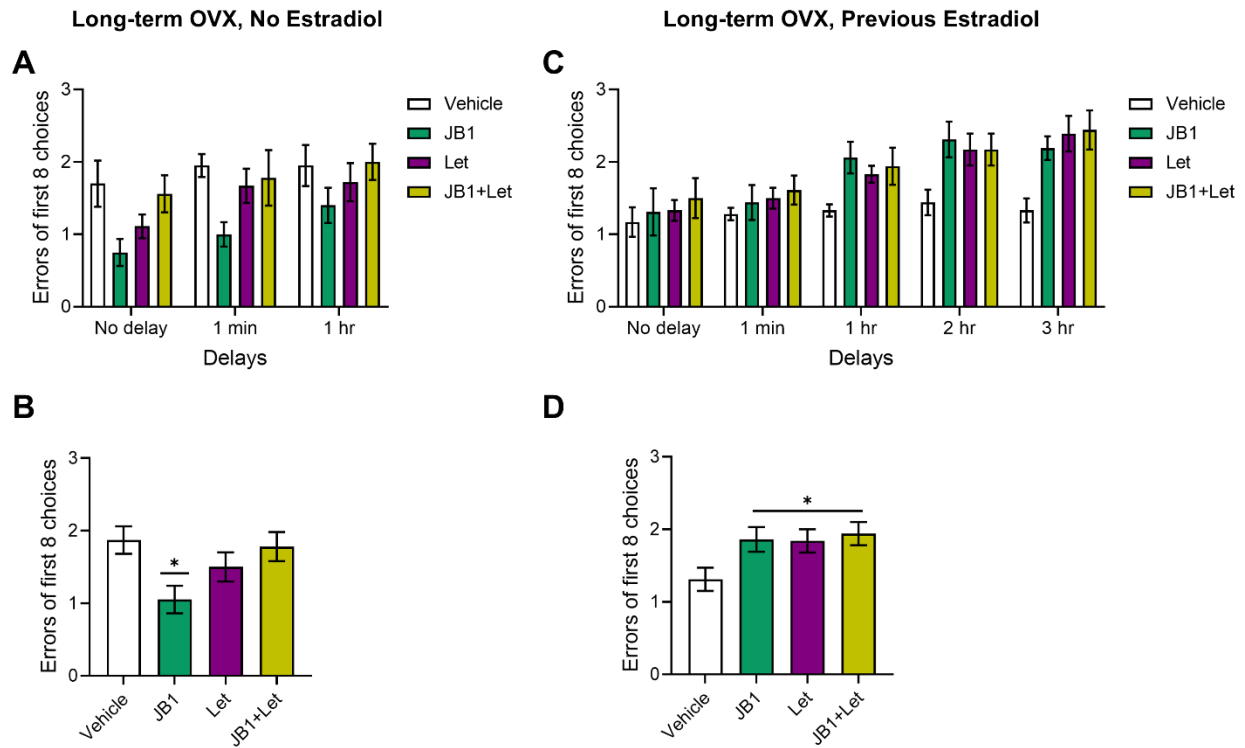
845

846

847 Figure 6

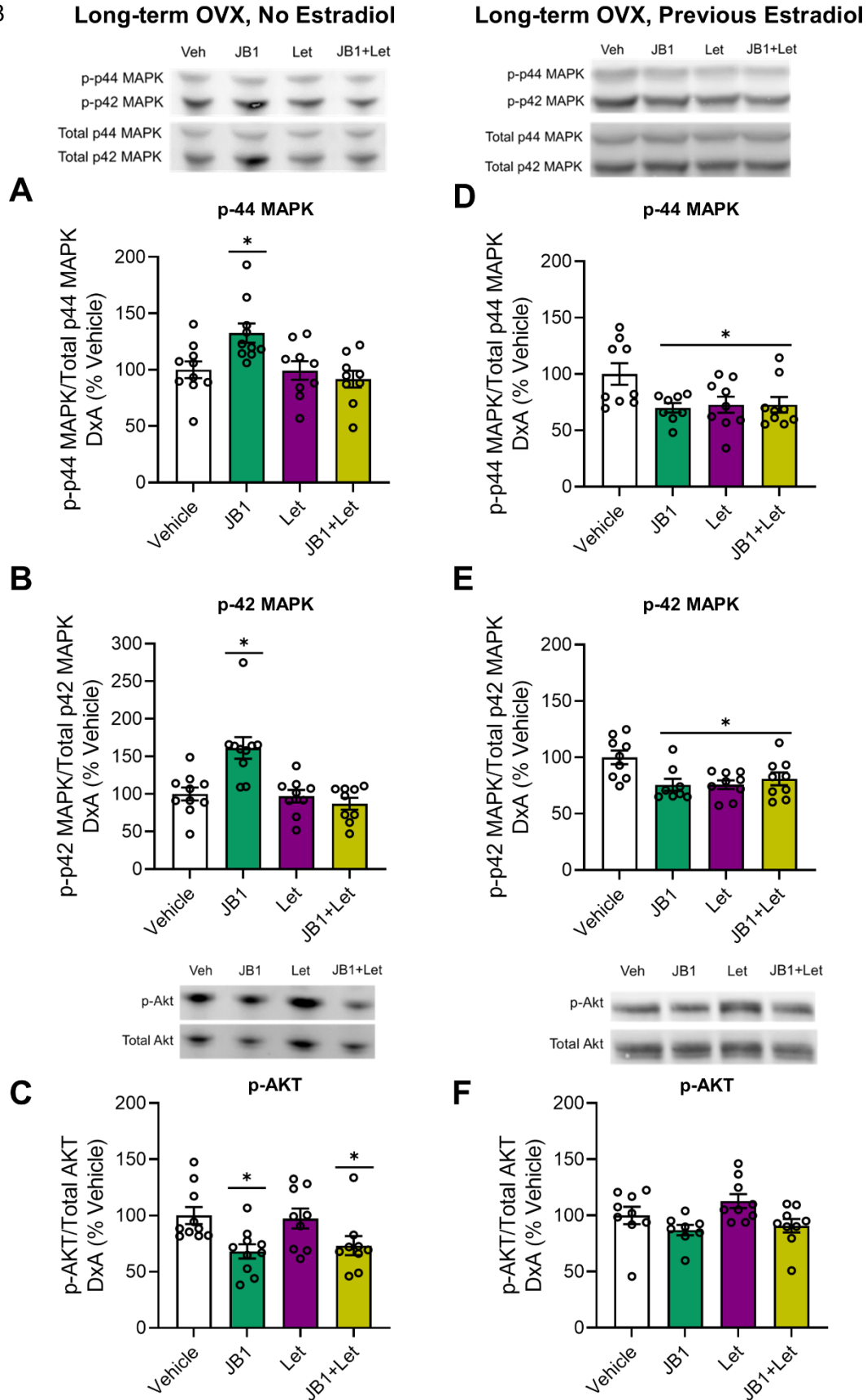


849 Figure 7

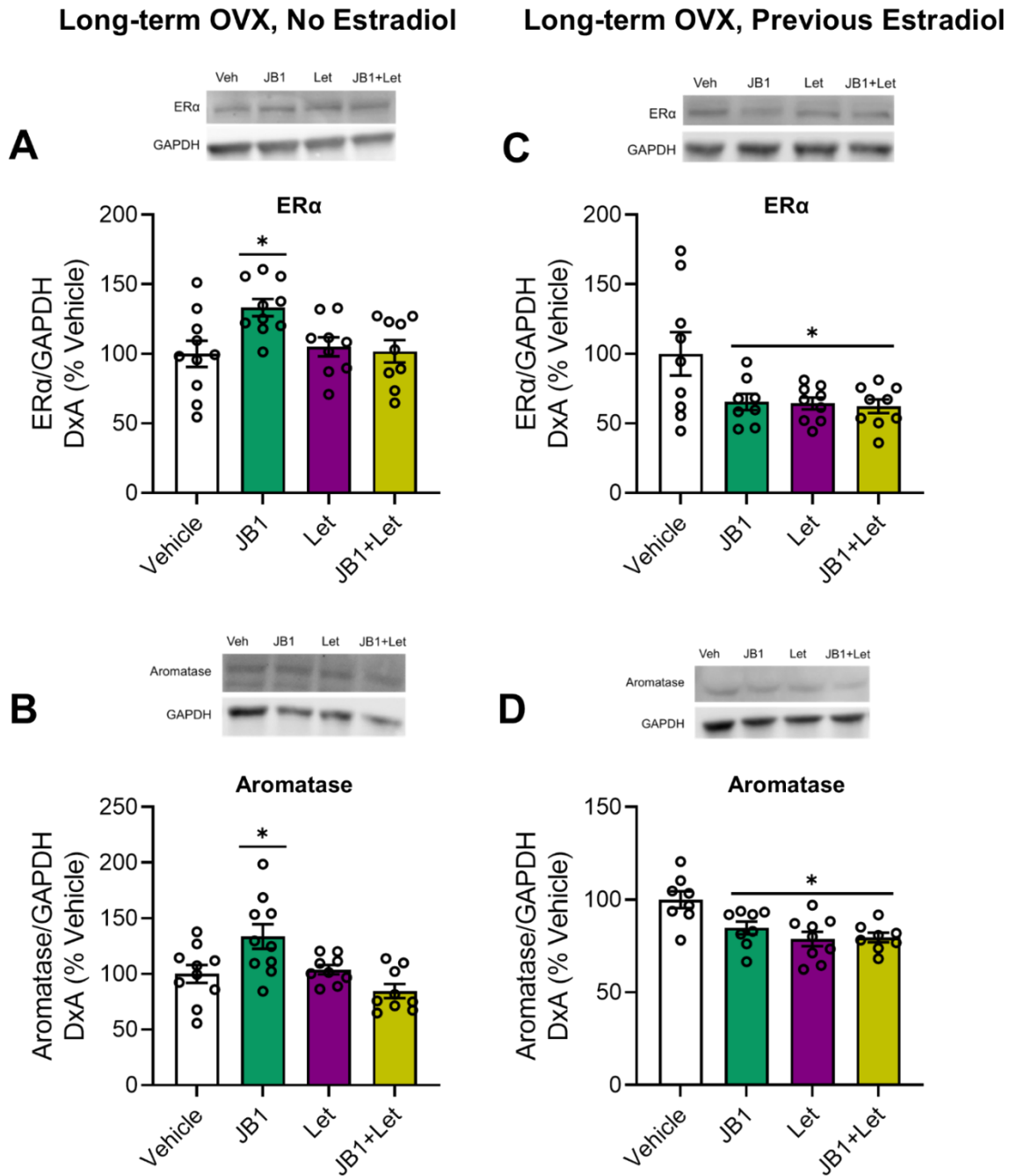


850

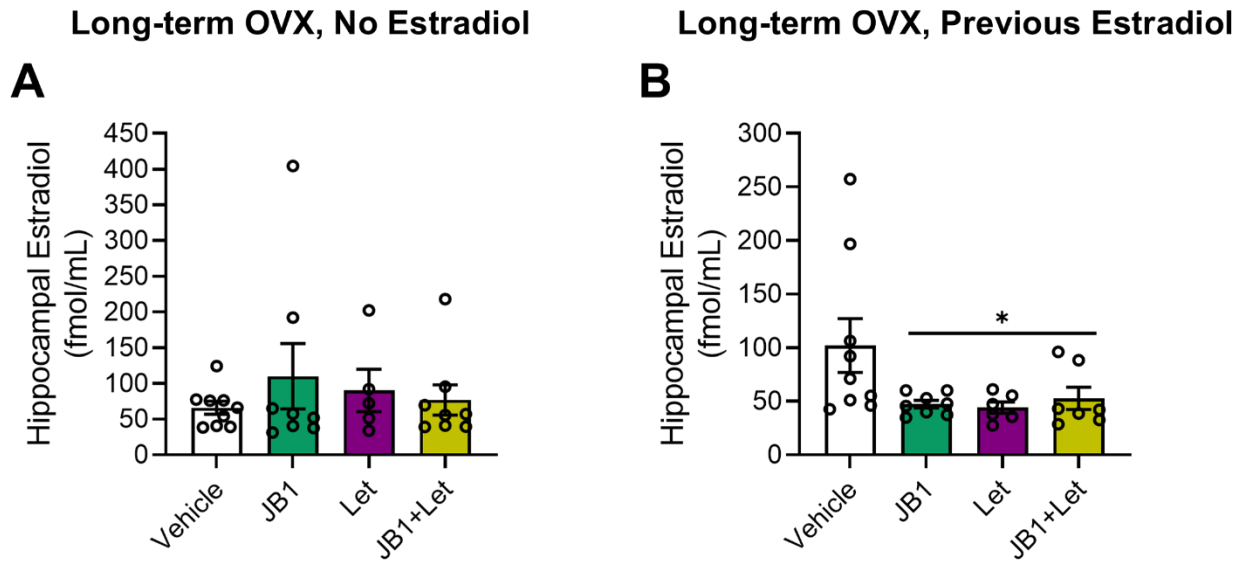
851 Figure 8



852 Figure 9



854 Figure 10



856 Figure Legends:

857 Figure 1. *Cytosolic expression of pS118-ER α and total ER α 1-hour or 24-hours post infusion of*
858 *IGF-1 or IGF-1 + letrozole in the hippocampus of ovariectomized rats.* Middle-aged female rats
859 were ovariectomized and given an acute infusion of either vehicle (Veh), insulin-like growth
860 factor-1 (IGF-1), or IGF-1 and the aromatase inhibitor letrozole (IGF-1 + Let) to the lateral
861 ventricle. Either 1 or 24-hours later, hippocampi were processed for subcellular fractionation and
862 western blotting for phosphorylated levels of ER α at S118 (pS118-ER α), total ER α , and
863 cytosolic loading control enolase in the cytosolic fraction of all samples. Levels of pS118 were
864 normalized to total ER α levels % vehicle group, and levels of total ER α were normalized to
865 enolase % vehicle group. A) There was an effect of treatment ($p < 0.05$) on pS118-ER α levels in
866 the cytosol compartment 1-hour post infusion, with post hoc testing revealing increased levels in
867 the IGF-1 group as compared to vehicle group. B-D) There was no effect of treatment on
868 pS118-ER α levels 24-hours post infusion (B), nor was there an effect of treatment on total ER α
869 levels either 1-hour (C) or 24-hours (D) post infusion. * $p < 0.05$ vs. Veh

870

871 Figure 2. *Membrane expression of pS118-ER α and total ER α 1-hour or 24-hours post infusion*
872 *of IGF-1 or IGF-1 + letrozole in the hippocampus of ovariectomized rats.* Middle-aged female
873 rats were ovariectomized and given an acute infusion of either vehicle (Veh), insulin-like growth
874 factor-1 (IGF-1), or IGF-1 and the aromatase inhibitor letrozole (IGF-1 + Let) to the lateral
875 ventricle. Either 1 or 24-hours later, hippocampi were processed for subcellular fractionation and
876 western blotting for phosphorylated levels of ER α at S118 (pS118-ER α), total ER α , and
877 membrane loading control ATP1A1 in the membrane fraction of all samples. Levels of pS118-
878 ER α were normalized to total ER α levels % vehicle group, and levels of total ER α were
879 normalized to ATP1A1 % vehicle group. A-B) There was no effect of treatment on membrane

880 pS118-ER α levels either 1-hour (A) or 24-hours (B) post infusion. C-D) There was no effect of
881 treatment on membrane total ER α levels either 1-hour (C) or 24-hours (D) post infusion.

882

883 Figure 3. *Nuclear expression of pS118-ER α and total ER α 1-hour or 24-hours post infusion of*
884 *IGF-1 or IGF-1 + letrozole in the hippocampus of ovariectomized rats.* Middle-aged female rats
885 were ovariectomized and given an acute infusion of either vehicle (Veh), insulin-like growth
886 factor-1 (IGF-1), or IGF-1 and the aromatase inhibitor letrozole (IGF-1 + Let) to the lateral
887 ventricle. Either 1 or 24-hours later, hippocampi were processed for subcellular fractionation and
888 western blotting for phosphorylated levels of ER α at S118 (pS118-ER α), total ER α , and nuclear
889 loading control CREB in the nuclear fraction of all samples. Levels of pS118 were normalized to
890 total ER α levels % vehicle group, and levels of total ER α were normalized to CREB % vehicle
891 group. A-B) There was no effect of treatment on pS118-ER α levels in the nuclear compartment
892 either 1-hour (A) or 24-hours (B) post infusion. C) There was no effect of treatment on pS118-
893 ER α levels 24-hours post infusion. D) There was an effect of treatment ($p < 0.05$) on total ER α
894 levels 24-hours post infusion, with post hoc testing revealing increased levels in the IGF-1 group
895 as compared to the Veh group. * $p < 0.05$ vs. Veh

896

897 Figure 4. *Hippocampal MAPK and Akt pathway activation 1-hour or 24-hours post infusion of*
898 *IGF-1 or IGF-1 + letrozole.* Middle-aged female rats were ovariectomized and given an acute
899 infusion of either vehicle (Veh), insulin-like growth factor-1 (IGF-1), or IGF-1 and the aromatase
900 inhibitor letrozole (IGF-1 + Let) to the lateral ventricle. Either 1 or 24-hours later, hippocampi
901 were processed for western blotting for phosphorylated and total levels of p44-MAPK, p42-
902 MAPK, and Akt. Phosphorylated levels were normalized to the total protein levels and
903 expressed as a percentage of the Veh group mean. A-D) One hour post infusion, there was a

904 main effect of treatment ($p < 0.05$) on phosphorylated levels of p44-MAPK (A) and p42-MAPK
905 (B), with post hoc testing revealing increased phosphorylation of both MAPK phosphorylation
906 sites in the IGF-1 group as compared to the Veh group. There was no effect of treatment on
907 phosphorylated levels of p44-MAPK (D) or p42-MAPK (E) 24-hours post infusion. C) One hour
908 post infusion, there was an effect ($p < 0.05$) of treatment on phosphorylated levels of Akt, with
909 post hoc testing revealing increased levels in both the IGF-1 and IGF-1 + Let groups as
910 compared to the Veh group. F). There was no effect of treatment on phosphorylated levels of
911 Akt 24-hours post infusion. * $p < 0.05$ vs. Veh

912

913 Figure 5. *Impacts of chronic IGF-1 or IGF-1 + Letrozole treatment on performance on the*
914 *hippocampal-dependent radial-arm maze task.* Middle-aged female rats were trained on the 8-
915 arm radial maze task and subsequently ovariectomized and treated with either vehicle (Veh),
916 insulin-like growth factor-1 (IGF-1) or IGF-1 plus the aromatase inhibitor letrozole (IGF-1+Let)
917 and tested on the maze using delays of 1, 3, 4, and 5 hours. Data represent the number of
918 incorrect choices made in the first eight choices averaged across two days of testing at each
919 delay. A) There was a main effect of delay ($p < 0.05$) on performance across groups, with post
920 hoc testing revealing errors increased as delays became longer. There was no significant
921 interaction between delay x treatment. B) There was a main effect of treatment ($p < 0.05$) on
922 performance averaged across all delays, with post hoc testing revealing significantly fewer
923 errors in the IGF-1 group as compared to the Veh group. * $p < 0.05$ vs. Veh

924

925 Figure 6. *Impacts of chronic IGF-1 or IGF-1 + Letrozole treatment on hippocampal MAPK and*
926 *Akt pathway activation.* Middle-aged female rats were ovariectomized and treated with either
927 vehicle (Veh), insulin-like growth factor-1 (IGF-1) or IGF-1 plus the aromatase inhibitor letrozole

928 (IGF-1+Let). After rats were tested on the radial-arm maze, hippocampi were dissected and
929 processed for western blotting for phosphorylated and total levels of p44-MAPK, p42-MAPK,
930 and Akt. Phosphorylated levels were normalized to the total protein levels and expressed as a
931 percentage of the Veh group mean. There was an effect of treatment ($p<0.05$) on
932 phosphorylated levels of p44-MAPK (A) and p42-MAPK (B), with post hoc testing revealing
933 increased phosphorylation of both MAPK phosphorylation sites in the IGF-1 group as compared
934 to the Veh group. There was an effect of treatment ($p<0.05$) on phosphorylated levels of Akt (C),
935 with post hoc testing revealing increased phosphorylation in both the IGF-1 and IGF-1+Let
936 groups as compared to Veh group. * $p<0.05$ vs. Veh

937

938 *Figure 7. Impacts of chronic JB1, Letrozole, or JB1+Letrozole treatment on radial-arm maze*
939 *performance in long-term ovariectomized rats with or without previous midlife estradiol*
940 *exposure.* Middle-aged female rats were ovariectomized and immediately implanted with vehicle
941 (Long-term OVX, No Estradiol) or estradiol (Long-term OVX, Previous Estradiol) capsules. Forty
942 days later, capsules were removed. One-hundred days following loss of circulating estrogens
943 (either via ovariectomy in Long-term OVX, No Estradiol group or removal of estradiol capsule in
944 Long-term OVX, Previous Estradiol group), rats were trained on the 8-arm radial maze task and
945 Following training, rats were treated with chronic i.c.v. administration of either vehicle (Veh), the
946 IGF-1R antagonist JB1 (JB1), the aromatase inhibitor letrozole (Let), or JB1 and letrozole
947 (JB1+Let) and tested on the maze using delays (Long-term OVX, No Estradiol: No Delay, 1
948 minute, and 1 hour; Long-term OVX, Previous Estradiol: No Delay, 1 minute, 1 hour, 2 hour, and
949 3 hour). Data represent the number of incorrect choices made in the first eight choices averaged
950 across two days of testing at each delay. A) Following long-term ovariectomy with no estradiol
951 exposure, there was a main effect of delay ($p<0.05$) on performance across groups, with post
952 hoc testing revealing errors increased as delays became longer. There was no significant

953 interaction between delay x treatment. B) There was a main effect of treatment ($p<0.05$) on
954 performance averaged across all delays following long-term ovariectomy with no estradiol, with
955 post hoc testing revealing significantly fewer errors in the JB1 group as compared to the Veh
956 group. C) Following long term ovariectomy with previous estradiol exposure, there was a main
957 effect of delay ($p<0.05$) on performance across groups, with post hoc testing revealing errors
958 increased as delays became longer. There was no significant interaction between delay x
959 treatment. D) There was a main effect of treatment ($p<0.05$) on performance averaged across
960 all delays following previous estradiol exposure, with post hoc testing revealing significantly
961 more errors in the JB1, Let, and JB1+Let groups as compared to the Veh group. $*p<0.05$ vs.
962 Veh

963

964 *Figure 8. Impacts of chronic JB1, Letrozole, or JB1+Letrozole treatment on hippocampal MAPK*
965 *and Akt pathway activation in long-term ovariectomized rats with or without previous midlife*
966 *estradiol exposure.* Middle-aged female rats were ovariectomized and immediately implanted
967 with vehicle (Long-term OVX, No Estradiol groups) or estradiol (Long-term OVX, Previous
968 Estradiol groups) capsules. Forty days later, capsules were removed. One-hundred days
969 following loss of circulating estrogens (either via ovariectomy in Long-term OVX, No Estradiol
970 group or removal of estradiol capsule in Long-term OVX, Previous Estradiol group), rats were
971 trained on the 8-arm radial maze task and subsequently treated with chronic i.c.v. administration
972 of either vehicle (Veh), the IGF-1R antagonist JB1 (JB1), the aromatase inhibitor letrozole (Let),
973 or JB1 and letrozole (JB1+Let). After rats were tested on the radial-arm maze, hippocampi were
974 dissected and processed for western blotting for phosphorylated and total levels of p44-MAPK,
975 p42-MAPK, and Akt. Phosphorylated levels were normalized to the total protein levels and
976 expressed as a percentage of the Veh group mean. Following long-term ovariectomy with no
977 estradiol exposure, there was an effect of treatment ($p<0.05$) on phosphorylated levels of p44-

978 MAPK (A) and p42-MAPK (B), with post hoc testing revealing increased phosphorylation of both
979 MAPK phosphorylation sites in the JB1 group as compared to the Veh group. There was also an
980 effect of treatment ($p<0.05$) on phosphorylated levels of Akt (C), with post hoc testing revealing
981 decreased phosphorylation in both the JB1 and JB1+Let groups as compared to Veh group.
982 Following long-term ovariectomy with previous estradiol exposure, there was an effect of
983 treatment ($p<0.05$) on phosphorylated levels of p44-MAPK (D) and p42-MAPK (E), with post
984 hoc testing revealing decreased phosphorylation of both MAPK phosphorylation sites in the
985 JB1, Let, and JB1+Let groups as compared to the Veh group. There was also an effect of
986 treatment ($p<0.05$) on phosphorylated levels of Akt (F), with post hoc testing revealing no
987 significant difference between the treatment groups and the Veh group. * $p<0.05$ vs. Veh

988

989 *Figure 9. Impacts of chronic JB1, Letrozole, or JB1+Letrozole treatment on hippocampal ER α*
990 *and aromatase levels in long-term ovariectomized rats with or without previous midlife estradiol*
991 *exposure.* Middle-aged female rats were ovariectomized and immediately implanted with vehicle
992 (Long-term OVX, No Estradiol groups) or estradiol (Long-term OVX, Previous Estradiol groups)
993 capsules. Forty days later, capsules were removed. One-hundred days following loss of
994 circulating estrogens (either via ovariectomy in Long-term OVX, No Estradiol group or removal
995 of estradiol capsule in Long-term OVX, Previous Estradiol group), rats were trained on the 8-
996 arm radial maze task and subsequently treated with chronic i.c.v. administration of either vehicle
997 (Veh), the IGF-1R antagonist JB1 (JB1), the aromatase inhibitor letrozole (Let), or JB1 and
998 letrozole (JB1+Let). After rats were tested on the radial-arm maze, hippocampi were dissected
999 and processed for western blotting for ER α , aromatase, and loading control GAPDH. ER α and
1000 aromatase levels were normalized to GAPDH levels and expressed as a percentage of the Veh
1001 group mean. Following long-term ovariectomy with no estradiol exposure, there was an effect of
1002 treatment ($p<0.05$) on hippocampal ER α (A) and aromatase (B) expression, with post hoc

1003 testing revealing increased levels of both proteins in the JB1 group as compared to the Veh
1004 group. Following long-term ovariectomy with previous estradiol exposure, there was an effect of
1005 treatment ($p < 0.05$) on hippocampal ER α (C) and aromatase (D) expression with post hoc
1006 testing revealing decreased levels in the JB1, Let, and JB1+Let groups as compared to the Veh
1007 group. * $p < 0.05$ vs. Veh

1008

1009 *Figure 10. Impacts of chronic JB1, Letrozole, or JB1+Letrozole treatment on hippocampal*
1010 *estradiol levels in long-term ovariectomized rats with or without previous midlife estradiol*
1011 *exposure.* Middle-aged female rats were ovariectomized and immediately implanted with vehicle
1012 (Long-term OVX, No Estradiol groups) or estradiol (Long-term OVX, Previous Estradiol groups)
1013 capsules. Forty days later, capsules were removed. One-hundred days following loss of
1014 circulating estrogens (either via ovariectomy in Long-term OVX, No Estradiol group or removal
1015 of estradiol capsule in Long-term OVX, Previous Estradiol group), rats were trained on the 8-
1016 arm radial maze task and subsequently treated with chronic i.c.v. administration of either vehicle
1017 (Veh), the IGF-1R antagonist JB1 (JB1), the aromatase inhibitor letrozole (Let), or JB1 and
1018 letrozole (JB1+Let). After rats were tested on the radial-arm maze, hippocampi were dissected
1019 and processed for estradiol detection via UPLC-MS/MS. Estradiol levels are expressed in
1020 fmol/mL. A) Following long-term ovariectomy with no estradiol exposure, there was no effect of
1021 treatment on hippocampal estradiol levels. B) Following long-term ovariectomy with previous
1022 estradiol exposure, there as an effect of treatment ($p < 0.05$) on estradiol levels, with post hoc
1023 testing revealed decreased levels in the JB1, Let, and JB1+Let groups as compared to the Veh
1024 group. * $p < 0.05$ vs. Veh